JOURNAL OF GEOPHYSICAL RESEARCH, VOL. 101, NO. B5, PAGES 11,173–11,194, MAY 10, 1996

Crustal structure of the Colorado Plateau, Arizona: Application of new long-offset seismic data analysis techniques

Tom Parsons,[1] Jill McCarthy,[1] William M. Kohler,[1] Charles J. Ammon,[2] Harley M. Benz,[3] J. A. Hole,[4] and Edward E. Criley[1]

Abstract. The Colorado Plateau is a large crustal block in the southwestern United States that has been raised intact nearly 2 km above sea level since Cretaceous marine sediments were deposited on its surface. Controversy exists concerning the thickness of the plateau crust and the source of its buoyancy. Interpretations of seismic data collected on the plateau vary as to whether the crust is closer to 40 or 50 km thick. A thick crust could support the observed topography of the Colorado Plateau isostatically, while a thinner crust would indicate the presence of an underlying low-density mantle. This paper reports results on long-offset seismic data collected during the 1989 segment of the U.S. Geological Survey Pacific to Arizona Crustal Experiment that extended from the Transition Zone into the Colorado Plateau in northwest Arizona. We apply two new methods to analyze long-offset data that employ finite difference travel time calculations: (1) a first-arrival time inverter to find upper crustal velocity structure and (2) a forward-modeling technique that allows the direct use of the inverted upper crustal solution in modeling secondary reflected arrivals. We find that the crustal thickness increases from 30 km beneath the metamorphic core complexes in the southern Basin and Range province to about 42 km beneath the northern Transition Zone and southern Colorado Plateau margin. We observe some crustal thinning (to ~37 km thick) and slightly higher lower crustal velocities farther inboard; beneath the Kaibab uplift on the north rim of the Grand Canyon the crust thickens to a maximum of 48 km. We observe a nonuniform crustal thickness beneath the Colorado Plateau that varies by ~15% and corresponds approximately to variations in topography with the thickest crust underlying the highest elevations. Crustal compositions (as inferred from seismic velocities) appear to be the same beneath the Colorado Plateau as those in the Basin and Range province to the southwest, implying that the plateau crust represents an unextended version of the Basin and Range. Some of the variability in crustal structure appears to correspond to preserved lithospheric discontinuities that date back to the Proterozoic Era.

Introduction

The crustal thickness beneath the Colorado Plateau has been a recent source of controversy. Early seismic refraction experiments conducted on the plateau found intermediate crustal thicknesses of 40–43 km [*Roller*, 1965; *Warren*, 1969]. *Prodehl* [1979] reinterpreted the *Roller* [1965] study and also concluded that the crust was 40–43 km thick. *Hauser and Lundy* [1989] combined new deep seismic reflection data recorded on the Colorado Plateau with a reinterpretation of the *Roller* [1965] and *Warren* [1969] data to suggest that the plateau crust is at least 50 km thick. *Wolf and Cipar* [1993] interpreted the crust in the vicinity of the Grand Canyon to be 45 (±3) km thick. *Pn* velocities of 7.8 km/s were reported by *Roller* [1965] and *Warren* [1969] and were based on reversed refraction profiles.

In 1985 the U.S. Geological Survey (USGS) initiated a deep crustal seismic investigation of the Colorado Plateau–southern Basin and Range transition. This study, referred to as the Pacific to Arizona Crustal Experiment (PACE), incorporates seismic refraction methods to constrain rock composition and crustal and upper mantle structure. The seismic refraction studies were initiated in 1985 midway along the PACE transect [*Wilson and Fuis*, 1987; *Wilson et al.*, 1991] and were extended to the northeast across the Transition Zone in 1987 [*Larkin et al.*, 1988; *McCarthy et al.*, 1991]. In September of 1989 the USGS, in conjunction with the University of Texas at El Paso, the University of Saskatchewan, the University of Arizona, the Air Force Geophysics Laboratory, Stanford University, and the Geological Survey of Canada, conducted a third seismic refraction experiment across the northeastern Transition Zone and the southwestern margin of the Colorado Plateau. This third segment of the transect provides insights into the crustal structure of the relatively unextended Colorado Plateau province and the change in crustal structure southwest toward the highly extended metamorphic core complexes (Figure 1).

This paper has two primary purposes. The first is to present results from the PACE 1989 seismic studies as they pertain to the crustal structure of the southwest margin of the Colorado Plateau in Arizona. The second goal is to introduce a new, unified approach to modeling crustal and upper mantle veloc-

[1]U.S. Geological Survey, Menlo Park, California.
[2]Department of Earth and Atmospheric Sciences, Saint Louis University, Saint Louis, Missouri.
[3]U.S. Geological Survey, Denver, Colorado.
[4]Department of Geophysics, Stanford University, Stanford, California.

Paper number 95JB03742.
0148-0227/96/95JB-03742$09.00

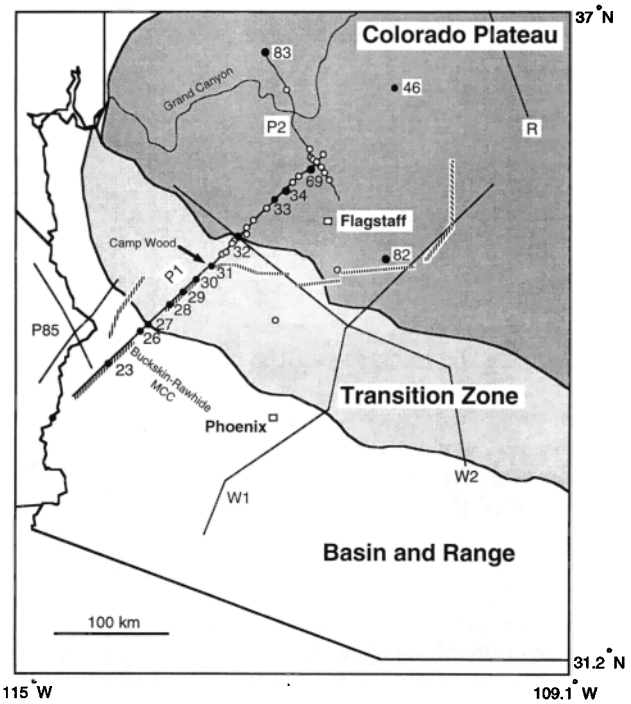

Figure 1a. Location of existing refraction (solid black) and Consortium for Continental Reflection Profiling reflection (vertical lined) profiles in the Arizona portion of the Colorado Plateau. Abbreviations are as follows: P1, Pacific to Arizona Crustal Experiment (PACE) Colorado Plateau profile; P2, PACE Grand Canyon profile; R, Arizona portion of *Roller* [1965] Hanksville-Chinle profile; W1, *Warren* [1969] Gila Bend-Surprise profile; and W2, *Warren* [1969] Blue Mountain-Bylass profile. Circles along the PACE refraction profiles represent shots recorded during the 1989 experiment; solid circles represent those shots that recorded a Moho reflection. The subsurface coverage resulting from these shots is shown in Figure 9b. The abbreviation MCC stands for metamorphic core complex on this and following figures.

ity structure using finite difference travel time calculations. Our motivation for developing and applying new techniques for long-offset seismic data analysis was to find a fast, accurate way to invert for upper crustal velocity structure in regions with strong lateral-velocity contrasts and immediately apply the results into a model for the lower crust without translating or adapting the inverted solution. Solving for upper crustal velocity structure by conventional ray-tracing methods can be the most time-intensive and tedious part of interpreting long-offset data, and translating results from existing inversion schemes into forward layer-based modeling methods can also be time-consuming and result in a loss of detail. We include an interpretation of the 1987 PACE data using the new methods discussed above as a way to test and compare results from the finite difference techniques with results from ray-tracing methods. The 1987 and 1989 profiles were adjoining, and some shot points were used during both experiments. We thus found it useful in interpreting the new 1989 data to model both profiles together.

Description of the Experiment and Resulting Data

Two refraction/wide-angle reflection profiles were acquired during the 1989 PACE experiment (Figure 1). The first profile, referred to as the Colorado Plateau profile [*McCarthy et al.*, 1994], was oriented NE–SW and extended 150 km from the northeastern end of the 1987 PACE study, across Chino Valley, Arizona, to the western edge of the Navajo Indian Reservation, near Cameron, Arizona. This profile crossed the northeastern half of the Transition Zone and the southwestern margin of the Colorado Plateau. The average instrument spacing along this profile was 333 m, and the average shot spacing was 10 km. A total of 24 shots were recorded; three of these shots were offset to the southwest of the recording line, and one was offset to the northeast (Figure 1).

The second refraction profile, referred to as the Grand Canyon profile [*McCarthy et al.*, 1994], was oriented NW–SE and was situated strictly within the Colorado Plateau physiographic province (Figure 1). This profile intersected the Colorado Plateau profile on its northern end and was positioned as far inboard into the plateau as possible to constrain crustal thickness while avoiding the plateau margin, where extensional processes may have modified crustal structure. Ten in-line shots were recorded into this 150-km-long line; one of these shots was offset 75 km south of the recording array, resulting in maximum shot-receiver offsets of 225 km [*McCarthy et al.*, 1994].

The crustal and upper mantle velocity structure for the two PACE refraction profiles was derived from four major seismic phases: refracted arrivals from the upper crust (Pg) and upper mantle (Pn) and reflected phases from a middle crustal horizon (PiP) and the Moho (PmP). The middle crustal reflection (PiP) was observed on 11 shots on the Colorado Plateau profile and provided primary control for the velocity between 5 and 20 km depth. The reflection from the crust-mantle boundary (PmP) was observed on eight shots on the Colorado Plateau profile and two shots on the Grand Canyon profile. This phase provided control on estimates of lower crustal velocity and crustal thickness. Pn refractions were observed on five long-offset shots and provide control on upper mantle velocities only across the Transition Zone and the southwest margin of the plateau.

We observed a systematic decline in the signal-to-noise ratio northward along the transect corresponding to the tectonic subprovinces defined as southern Basin and Range, the Transition Zone, and the Colorado Plateau (Figure 1) [*McCarthy et al.*, 1994]. Data recorded within the southern Basin and Range and Transition Zone tend to show bright, clean reflected phases that are easy to identify (e.g., shot 23, Figure 2). Phases recorded northward toward the Colorado Plateau, however, have lower apparent amplitudes, and the phases are obscured

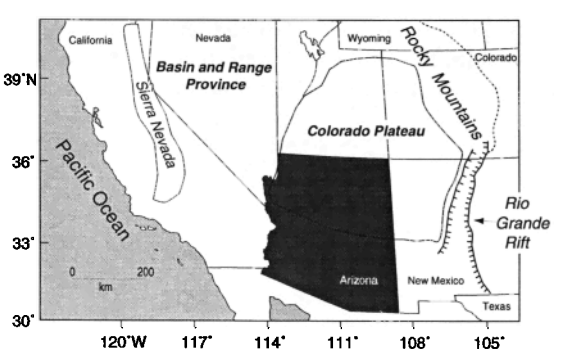

Figure 1b. Location of Colorado Plateau in relation to tectonic provinces of the Western Cordillera.

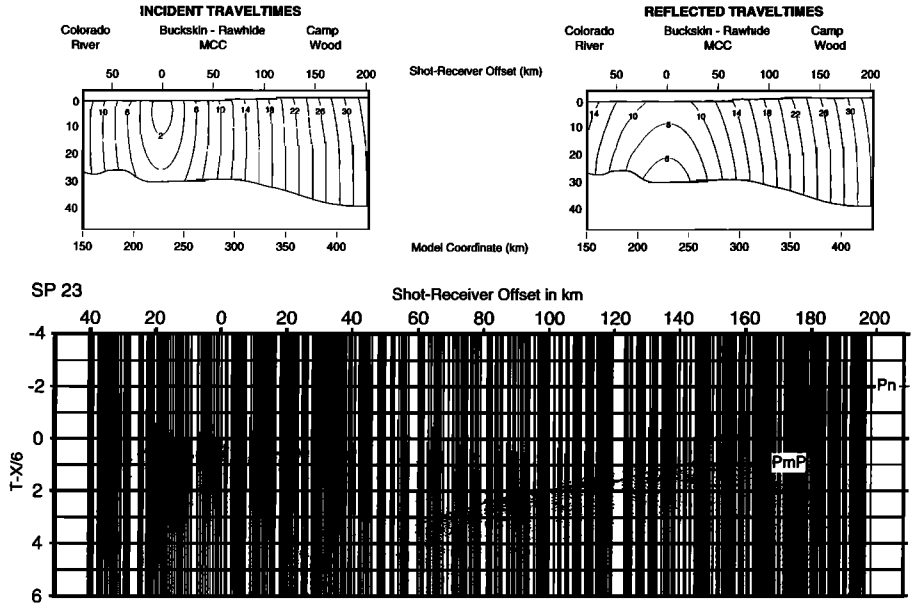

Figure 2. Shot record from shot 23, the furthest southwest off-end shot point in the PACE 1989 experiment (Figure 1). This shot was fired during both the PACE 1987 and 1989 experiments and is shown merged with the 1987 data. Heavy black line on the data shows the calculated reflection travel times for the Moho reflection (*PmP*). Above the data plot are contours of transmitted and reflected travel times calculated using the forward modeling package for calculating finite difference reflected travel times developed by *Hole and Zelt* [1995].

by increased background noise (e.g., *PmP* phases on shots 33, 34, and 46, Figures 3 and 4). The data quality decline into the Colorado Plateau because surface conditions (volcanic rocks and gravels) resulted in poor shot and receiver coupling [*McCarthy et al.*, 1994].

Modeling Methods

We assessed the seismic velocity of the crust and upper mantle along the PACE long-offset seismic profiles using three complementary methods. A finite difference tomographic inversion method was used to analyze refracted arrivals traveling through the upper crust (*Pg*). We then extended our velocity model downward into the middle and lower crust by employing a finite difference technique to forward model the propagation of seismic energy down to, and back up from, a reflecting interface at depth. By incorporating the inverted solution for upper crustal velocity in our grid, we were able to accurately model the effects of near-surface upper crustal structures (i.e., basins) on the arrival times of secondary arrivals. As a final step we used a finite difference solution to the acoustic wave equation to model the character and amplitudes of long-offset arrivals. This allowed us to test the nature of velocity discontinuities at depth. We discuss aspects of the inverse imaging techniques in some detail below, since they are not described elsewhere in the literature. Later in the text, after presentation of the seismic velocity models, we discuss the errors associated with these modeling techniques as applied to the Colorado Plateau data.

First-Arrival Travel Time Inversion for Upper Crustal Velocity Structure

The shallow fraction of the crust along the PACE profiles is very heterogeneous, particularly across the metamorphic core complex belt and the Transition Zone of the Colorado Plateau. Velocity variations of the order of 50%–100% occur across distances of a few kilometers [*McCarthy et al.*, 1991]. This dramatic structural variation makes for a time-consuming analysis of upper crustal velocity structure while also complicating the modeling of the deeper structure; tomographic inversion methods are thus the most effective means to analyze this complex portion of the velocity model. Any seismic tomography procedure requires an ability to compute travel times and/or ray paths, stabilize and invert a large set of algebraic equations, and assess model reliability. We discuss these three aspects of the tomography problem separately.

Computing travel times and ray paths. The computation of travel times is prerequisite to inverting observed travel times and thereby estimating the subsurface structure. We employ a finite difference travel time technique initially developed by *Vidale* [1988] and since extended by *Vidale* [1990] to perform more accurately in the presence of large velocity contrasts. In *Vidale*'s [1988] method, travel times are extrapolated outward from the source region to each point in the model (described by a finite difference mesh). To handle structures with large velocity contrasts, *Vidale* [1990] added a recursive element to the algorithm that searches for refracting waves which may have been overlooked in the original algorithm. The resulting algorithm more accurately times refracted and turning waves for a moderate increase in computation time. Ray paths are computed by following the gradient in travel time from the receiver to the source. To account for the large changes in elevation along the profiles (about 2 km of relief), we position the sources and receivers within a two-dimensional model, which is easily accommodated in the finite difference grid. Most often, a receiver will not be located on a grid point of the model, so the arrival time to a receiver is estimated using

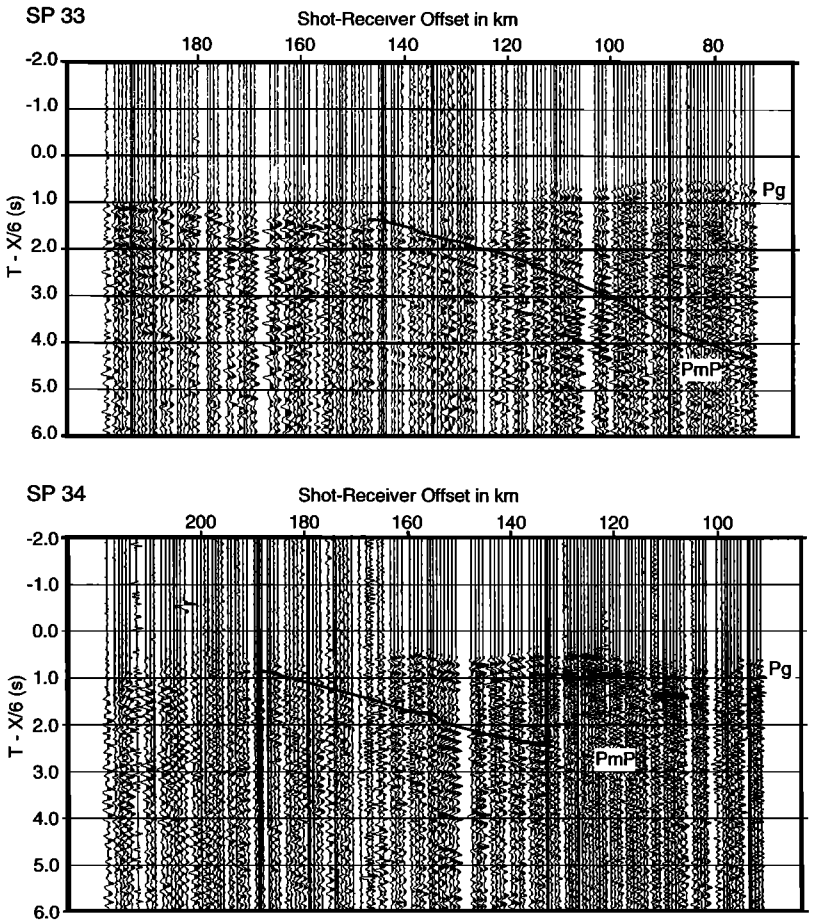

Figure 3. Partial shot records from shots 33 and 34 detonated on the Colorado Plateau (Figure 1). Moho reflections are discernible but are of lower apparent amplitude than the *PmP* reflections recorded in the Basin and Range or Transition Zone provinces (Figures 2 and 7). The weaker *PmP* reflections are probably a result of poor shot and receiver coupling on the Colorado Plateau. Calculated travel times are shown plotted on the data.

plane-wave interpolation of the times surrounding the receiver.

Nonlinear inversion of arrival times for subsurface slowness. The relationship between a medium's slowness (inverse of velocity) distribution and a wave travel time is nonlinear. Although the forward problem (computing times when given a velocity structure) may be solved with a number of approaches, solving the inverse problem (estimating the structure given a set of observed times) is more difficult. In media with small slowness variations the relationship can be linearized using Fermat's principle, resulting in a much simpler mathematical relationship. Unfortunately, because of the strongly heterogeneous uppermost crust along the PACE profiles, we cannot directly employ this simplification. We can, however, adopt the common approach of solving the nonlinear travel time equations iteratively, using Fermat's principle in successive iterations to linearize each step toward a solution of the nonlinear problem. Clearly, in this iterative scheme the initial velocity model plays an important role. We tested initial one-dimensional velocity structures based on a priori information from other studies of the area or areas with similar geologic characteristics. We tried a range of reasonable initial models, and all converged to more or less the same slowness structure, which is described below in a subsequent section.

We discretize the velocity structure using constant slowness cells and represent the ith slowness model using a vector notation $\mathbf{s}_i$. At each iteration the relationship between the travel times and the slowness perturbation, $\delta\mathbf{s}_{i+1} = \mathbf{s}_{i+1} - \mathbf{s}_i$, is

$$\mathbf{L}_i\delta\mathbf{s}_{i+1} = \delta\mathbf{t}_i. \tag{1}$$

$\mathbf{L}_i$ and $\delta\mathbf{t}_i$ are the path matrix and residual vector calculated using model $\mathbf{s}_i$. In general, seismic tomography problems are undetermined and ill-conditioned, and the direct inversion of (1) is very sensitive to small errors in the data. To produce reasonable estimates of the slowness, we must incorporate either geologic information or limit the possible solution to a certain class of models, such as the set of smoothest candidate models. This additional information may be incorporated by appending constraint equations to the system of equations relating the data and the model. We use a Laplacian smoothness criterion [*Lees and Crosson*, 1989], and the constraint equation for the cell located at x, z is of the form

$$4s_{x,z} - s_{x-dx,z} - s_{x+dx,z} - s_{x,z-dz} - s_{x,z+dz} = 0 \tag{2}$$

where dx, and dz are the cell widths in the horizontal and vertical directions, respectively. Additionally, minimum length constraints are necessary since the smoothest model criterion alone is sometimes inadequate to stabilize an inversion. The importance of smoothness, minimum length, and fitting the

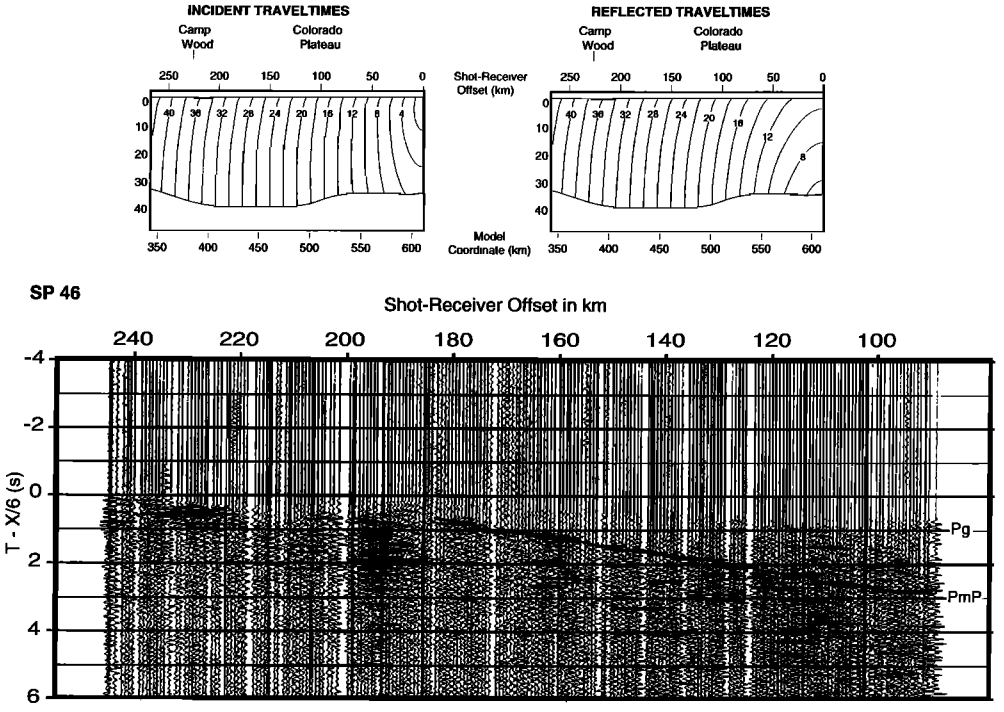

Figure 4. Shot record from shot 46, the northeastern off-end shot (Figure 1). Calculated travel times are shown on the data. A windowed plot of the *PmP* reflection from shot 46 without the calculated travel time curve is shown in Plate 1.

observed travel times are varied using a minimum length weight λ and a smoothing weight σ. The resulting equations are of the form

$$\begin{bmatrix} L_i \\ \sigma\Delta \\ \lambda I \end{bmatrix} \delta\mathbf{s}_{i+1} = \begin{bmatrix} \delta\mathbf{t}_i \\ 0 \\ 0 \end{bmatrix} \tag{3}$$

where L_i is a matrix of ray lengths and $\delta\mathbf{t}_i$ is the vector of travel time residuals both evaluated using slowness estimate $\mathbf{s}_i$, I is the identity matrix (with the dimensions of the slowness model), and Δ is a submatrix of Laplacian smoothness constraints. We solve (3) using the LSQR algorithm of *Paige and Saunders* [1982]. Appropriate values for λ and σ are estimated using a trial and error approach.

Resolution. Resolution in tomography depends on three properties of the problem. The signal band width, the source-receiver distribution, and the velocity structure itself. Three approaches are usually adopted to investigate resolution in tomographic problems. The simplest is a hit count analysis. In this simple analysis the number of rays sampling a given cell, or the sensitivity of all the travel times to each node, are examined to identify regions of good coverage (and hence good resolution is inferred) and poor coverage. The second approach to resolution analysis is the construction of synthetic tests using the data distribution [*Humphreys and Clayton*, 1988]. The synthetic test may be an attempt to construct point-spread functions or may be an attempt to reconstruct the major features of the model simultaneously. The third common method of resolution analysis is the use of the resolution matrix constructed from an extension of linear inverse theory. Typically, the diagonals of the resolution matrix are displayed, and a certain value is chosen to indicate "good" resolution. The resolution matrix is a construct well-suited to the study of linear problems. However, the extension of this tool to nonlinear problems is always questionable, particularly when the solution is approached iteratively [*Shaw and Orcutt*, 1986]. Each of the above resolution diagnostics depends on the velocity structure used to construct the resolution measures. Quantitatively connecting a hit count, synthetic test, or resolution matrix with the actual accuracy of the reconstructed image is not straight forward. A combination of these resolution indicators can provide some intuition into the resolving power of the data. We have chosen to use LSQR and thus do not construct a formal resolution matrix; we use a combination of hit count and synthetic tests to estimate the degree of uniqueness of the solution.

We can get a rough idea of the maximum resolution of the data by examining the Fresnel Zones. The Fresnel Zone is calculated by computing the travel time from the source to a point in the model and then on to the receiver. At the turning depth the Fresnel Zone is about 2 km wide, which indicates the practical limit on interpretation of the structure at depth. As expected, the Fresnel Zone is smaller at shallow depths where velocities are lower and resolution should be better in these regions, provided there is adequate sampling by the data. Figure 5 contains the coverage matrix for the final iterations of the inversions. The coverage for a node is calculated by summing the ray lengths of each ray path within a given cell.

Test of *Pg* inversion results. To test the travel time inversion method, we inverted the PACE 1987 travel time data and compared the results with the forward modeling results of *McCarthy et al.* [1991] (Figure 5). The inversion model was parameterized using 1-km cells. To maintain accuracy, a uniform grid point spacing of 200 m was employed for the travel time calculations. The final velocity models were obtained after five iterations. The travel time RMS decreased from 0.21 s (for a one-dimensional starting model) to 0.06 s for the model.

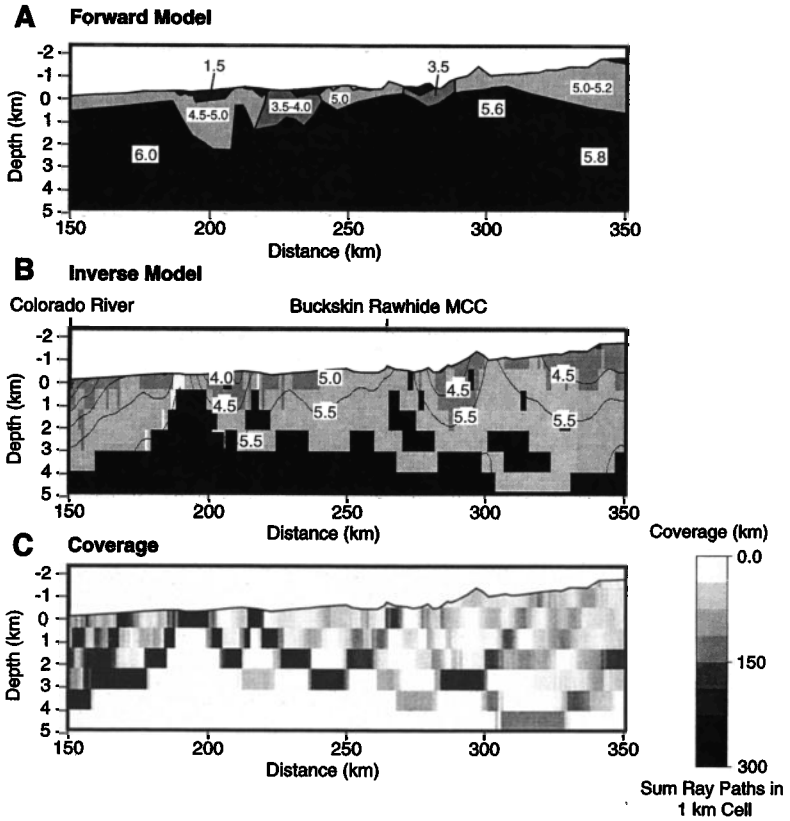

Figure 5. Comparison of upper crustal velocity structure across the PACE 1987 transect derived from (a) forward ray-tracing modeling [*McCarthy et al.*, 1991] and (b) finite difference tomographic inversion. (c) The ray coverage for the inversion is shown. Many of the primary features are present on both models such as low-velocity basins and higher velocities beneath the Buckskin-Rawhide metamorphic core complex. See further discussion in text.

The results of the travel time inversion for the upper 5 km of the crust across the 1987 transect are presented in Figure 5 and are compared to the forward ray-traced results of *McCarthy et al.* [1991]. The primary features of the velocity structure are evident in both models. The shallow basins in the region are well imaged by both methods, although some blurring in the vertical direction is observed on the tomographic inversion. Both methods also show an increase in velocity in the uppermost crust beneath the Buckskin-Rawhide metamorphic core complex, where low-angle normal faulting has stripped off the lower-velocity uppermost crust, exposing faster middle crustal rocks at the surface. The formal ray-tracing method has inherent discrete velocity boundaries, whereas the inverse model is discretized into small constant velocity cells. Velocity contrasts thus appear more smoothly varying in the inverted model. Given the close correspondence between the forward and inverse models, we are confident that the inversion technique properly determines the velocity structure of the upper crust. We therefore use this upper crustal solution in the analysis of secondary, reflected arrivals, as discussed below.

Finite Difference, Forward Modeling of Reflections

The finite difference travel time inversion used to find the upper crustal velocity structure utilizes only first-arrival times. To directly apply the inverted solution for the upper crust, we employed a finite difference technique to forward model crustal reflections, propagating though a velocity grid that contains the upper crustal model. We wrote the output from the first-arrival travel time inversion over a grid of input starting velocities, so that complexities in secondary phases that result from near-surface structures such as basins could be modeled as accurately as possible. Many of the shots recorded on the Colorado Plateau generated weak middle crustal reflections from a boundary approximately 17–20 km deep, as well as variable quality *PmP* reflections from the Moho. Thus we first treated the upper crustal velocity model from the travel time inversion as a known layer and solved for the velocity structure down to the middle crustal reflector. We then treated the model for the middle crustal horizon as a known layer and solved for the lower crustal velocities and whole crustal thickness.

The finite difference algorithm of *Vidale* [1988, 1990] is extended to compute reflection travel times [*Hole and Zelt*, 1995]. The technique was developed for use in three dimensions, although we apply it in only two dimensions in this study. The reflecting interface is defined as a sampled function of the horizontal coordinate and is allowed to vary smoothly in depth. To begin the procedure, first-arrival travel times are computed from the point source to the reflecting interface. Velocities below the reflector are defined to be equal to, or less than, velocities above in order to prevent waves transmitted through the interface from arriving as first arrivals at the reflector. The computed times at the reflecting interface are thus the times of the incident downgoing wave. To allow a smooth reflector to exist between grid nodes in depth, the computed incident times at the grid nodes immediately above the reflector are used to

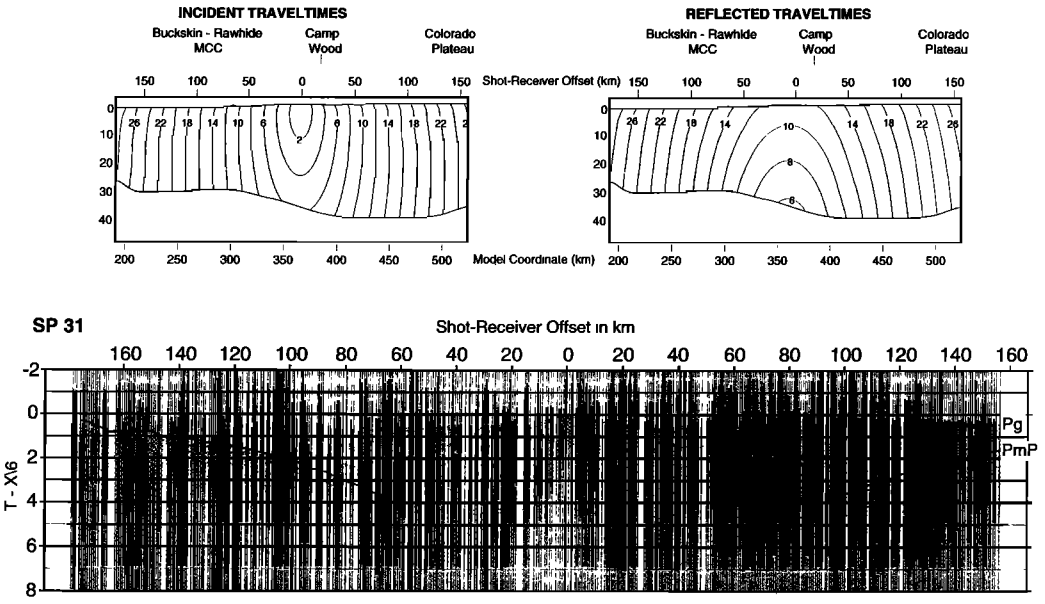

Figure 6. Shot record from shot 31 shown merged with the PACE 1987 data and displayed with calculated *PmP* travel times. A close-up of the *PmP* reflection recorded to the northeast is shown in Figure 11.

analytically compute reflected times at the same nodes. Travel times to shallower grid nodes are replaced with large dummy values. This sampled travel time field is input into the finite difference algorithm, and travel times are computed upward from the base of the model. Previously computed times (in particular the large dummy values) are replaced by upgoing times if the upgoing times are earlier. In this manner the incident travel times on the reflecting interface are used as a source to propagate the reflected wave upward through the model. In Figures 2, 3, 4, 6, and 8, contoured incident and reflected travel times are shown for reflections from the Moho and from a middle crustal horizon on reversing shots.

A Crustal Model for the Colorado Plateau Profile

We inverted the combined PACE 1987 and 1989 *Pg* travel time data to provide a complete upper crustal velocity grid (1-km cells) across the Transition Zone–Colorado Plateau physiographic provinces. Because the two profiles were adjoining, some shots were fired during both experiments, and thus an integrated analysis was desirable. A total of 6492 travel times were inverted to estimate the structure of the top 5–10 km of the crust. Figure 7 contains the results of our inversion. The final velocity models were obtained after five iterations. In addition to the features described above across the 1987 portion of the transect, several features are immediately apparent in the 1989 portion of the reconstruction.

Velocities in the shallow surface range from ~3.0 km/s at the tops of sedimentary basins to ~4.5 km/s across the Paleozoic limestones on the plateau. Velocities increase downward to ~6.0 km/s at a depth of only 2–3 km. Chino Valley, a shallow sedimentary basin, is resolved as a low-velocity feature (Figure 7), with velocities increasing from 3.0 to 4.5 km/s. Northeast of Chino Valley the Paleozoic sequence of limestone and sandstone beds can be seen thickening slightly toward the interior of the plateau (Figure 7). This northeastward thickening corresponds to an observed southwestward tapering of the Paleozoic section toward the plateau margin.

The deeper midcrustal structure was determined by analysis of relatively weak reflections recorded from 11 shots along the Colorado Plateau profile during the PACE 1989 experiment (Figures 8, 9). All 11 events were modeled as resulting from a single flat horizon at about 17 km depth (Figure 9). Travel times to this horizon constrain the velocity gradient in the upper crust, which we model as increasing from 5.9 km/s in the shallow crust (at the base of the *Pg* coverage) to 6.25 km/s at the top of the middle crustal reflector. The depth to this reflector and the velocities that underlie it (see discussion below) correlate well with the middle crustal reflector modeled by *McCarthy et al.* [1991] thus these horizons are connected on the combined 1987–1989 model (Figure 9).

The reflections from the middle crustal horizon arrive as a broad (multicyclic) phase in time (Figure 8). If we constrain the middle crustal reflector to be a single continuous horizon in depth, then the travel time residuals average about 0.22 s (larger than the average 0.05 s for the *PmP* reflection). Vertical incidence seismic reflection data coincident to the PACE profiles were acquired by the Consortium for Continental Reflection Profiling (COCORP) in 1986 [*Hauser et al.*, 1987] and by Stanford University in 1987 and in 1989 [*Goodwin and McCarthy*, 1990; *Howie et al.*, 1991]. These vertical-incidence data indicate a gradual increase in reflectivity between 16 and 20 km depth. The middle crustal reflector marks a textural division from a primarily transparent (to vertical-incidence seismic waves) upper crust into a variably reflective lower crust. It is thought from analysis of vertical-incidence reflection properties that the top of the zone of lower crustal reflectivity represents a collection of horizontal magmatic intrusions or sills [e.g., *Goodwin and McCarthy*, 1990; *Parsons et al.*, 1992; *McCarthy and Parsons*, 1994]. If some percentage of the lower crustal reflectivity results from mafic magmatic intrusions, then it is likely that the crustal velocity becomes faster beginning at the top of the lower crustal reflectivity; we have thus modeled this interface as a first-order velocity discontinuity. The relatively large travel time residuals that resulted in modeling this

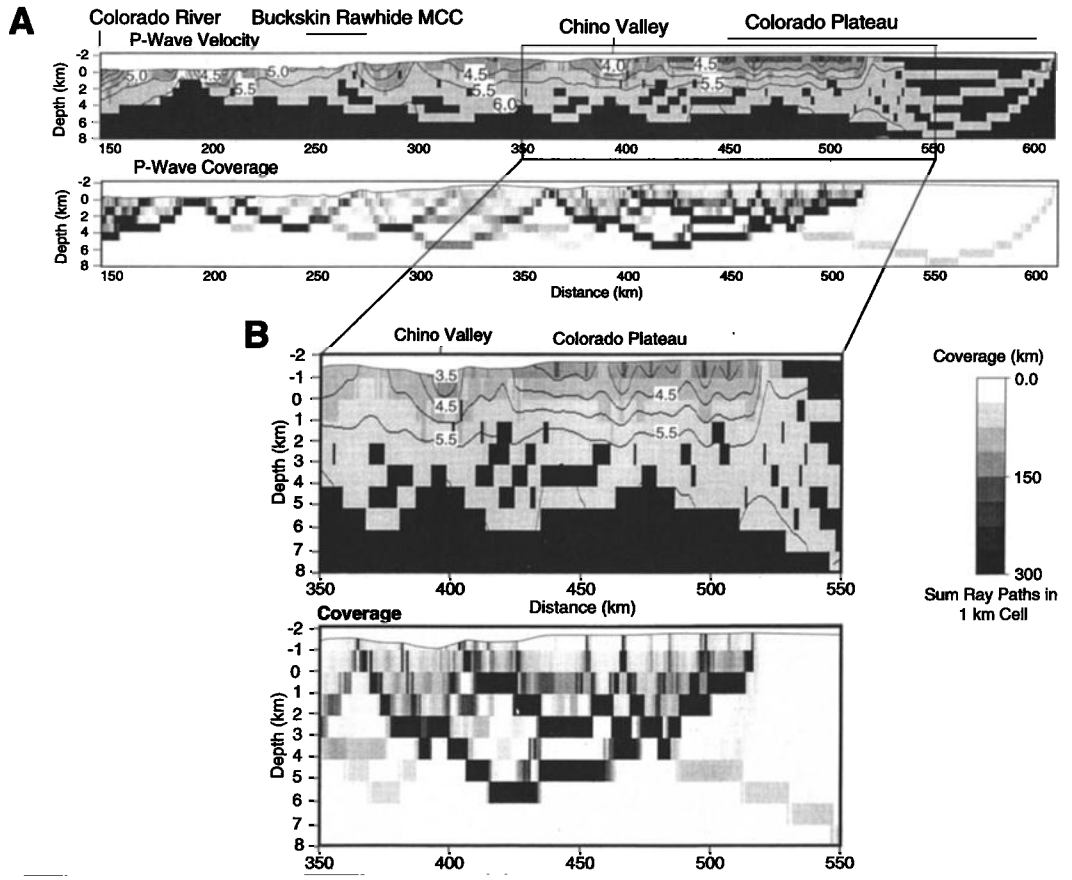

Figure 7. (a) Results from the travel time inversion for velocity structure of the upper crust on the PACE 1987 and 1989 profiles. (b) Close-up of the 1989 upper crustal velocity structure. Full discussion of the model features is in the text. Ray coverage for the inversion is shown beneath the velocity models.

horizon as a single reflector may be an indication that the middle crustal phase results from a transitional boundary characterized by horizontally discontinuous, alternating layers distributed over a 1- to 3-km-thick zone as seen in the vertical-incidence data.

The lower crustal velocity structure and crustal thickness across the transitional boundary of the Colorado Plateau are derived primarily from Moho (*PmP*) reflections recorded from eight shots along the Colorado Plateau profile (Figure 9). Calculated travel times for the *PmP* reflections are shown on representative data in Figures 2, 3, 4, and 6. The initial velocity of the lower crustal layer was taken from the adjoining PACE 1987 velocity model [*McCarthy et al.*, 1991]. Overall, this velocity (6.5–6.6 km/s) was successful in matching the *PmP* reflection curvature on the PACE 1989 profiles. At the northern end of the profile, slightly higher lower crustal velocities (6.5–6.8 km/s) (Figure 9) better matched the *PmP* reflection curvature of shot 46, the northern off-end shot (Figure 1). The bottoming points from this shot are beneath the edge of a Quaternary volcanic field, and it is possible that these high velocities are related to increased mafic magmatic input into the lower crust there, though the high velocities at the north end of the line are poorly constrained because they are only measured by one, unreversed shot (shot 46). The lower crustal layer thickens considerably from the 1987 to the 1989 profiles, which may be a result of varying tectonic extension along the transect. Beneath the highly extended Buckskin-Rawhide metamorphic core complex the lower crustal layer is about 5 km thick, while beneath the weakly to nonextended Transition Zone and Colorado Plateau margin the layer gradually thickens to a ~20–25 km thickness (Figure 9). We suggest that this lower crustal layer has been preferentially thinned by ductile flow during tectonic extension.

The crustal thickness increases from about 30 km beneath the Buckskin-Rawhide metamorphic core complex on the 1987 profile to a maximum of about 42 km thick beneath the northern Transition Zone and southern margin of the Colorado Plateau. We find that the crust may thin locally farther into the Colorado Plateau to about 37 km thick at the approximate longitude of Flagstaff (Figure 9), where lower crustal velocities are slightly faster (a thicker, slower crustal model did not adequately fit the *PmP* arrival from shot 46). The topography of the Colorado Plateau has often been referred to as "dish shaped" because the plateau edges are slightly higher than parts of its interior thus a slightly thinner crust away from the topographic edge might be expected if the plateau crust is partially isostatically compensated at the Moho.

A direct upper mantle phase (*Pn*) was recorded from five shots on the 1987 and 1989 profiles. The crustal model (Figure 9) was used as a starting model and was inverted for upper mantle velocity using *Pn* travel times, assuming an initial upper mantle velocity of 8.0 km/s. Slight variations from an 8.0 km/s velocity were found, but these did not exceed 0.1 km/s. The average (RMS) error for the *Pn* inversion was 0.15 s. When the cumulative uncertainties from the inverted upper crustal velocity structure and the forward middle and lower crustal

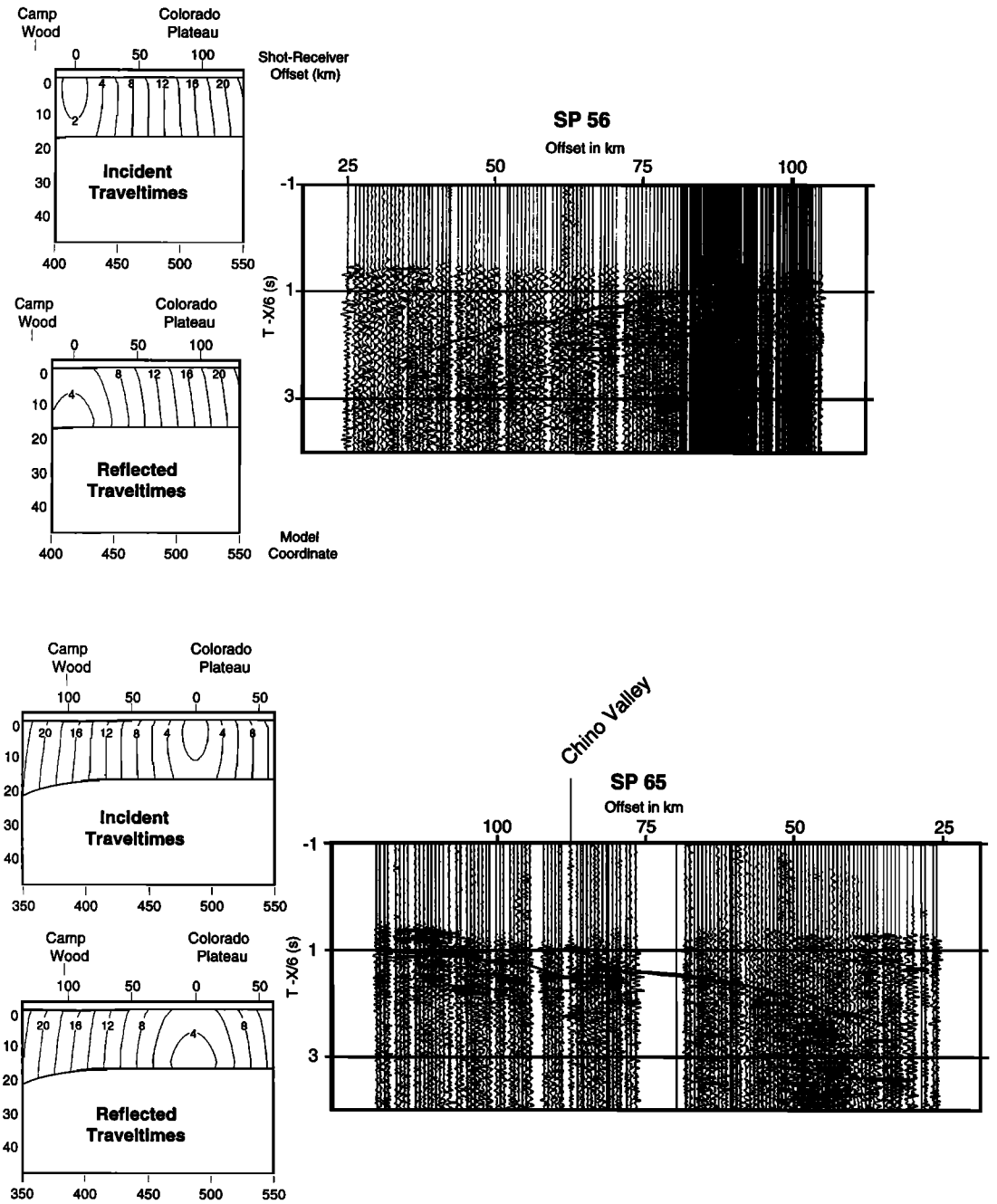

Figure 8. Partial shot records from shots 56 and 65 windowed to highlight the middle crustal reflections. Calculated travel times are shown on the data. The kink in the reflection from shot 65 is a delay from Chino Valley, a sedimentary basin adjacent to the physiographic edge of the Colorado Plateau (not seen on shot 56 because it was located ~5 km north of Chino Valley).

model are considered, the 0.1 km/s variations are insignificant, and we conclude that the upper mantle beneath the 1987 and 1989 profiles has an 8.0 km/s velocity. No *Pn* arrivals were recorded from beneath the Colorado Plateau on the PACE 1989 profiles, although *Warren* [1969] did observe *Pn* arrivals from beneath the plateau edge farther to the southeast. Difficult surface conditions may have obscured the low-amplitude *Pn* arrivals on the 1989 PACE profiles (further discussion on relative amplitudes of the *Pn* phase and ambient noise is presented in the Grand Canyon model section).

PmP Amplitude Models From Finite Difference Solutions of the Acoustic Wave Equation

We have modeled the Moho as a first-order velocity discontinuity from ~6.6 to 8.0 km/s (Figure 9). We tested this simple model of the Moho by applying a finite difference solution to the acoustic wave equation to see if it predicts appropriate *PmP* reflection character and amplitudes that match the data or whether more complex structures such as the magmatic layering proposed by *Wilshire* [1990] and *Wolf and Cipar* [1993]

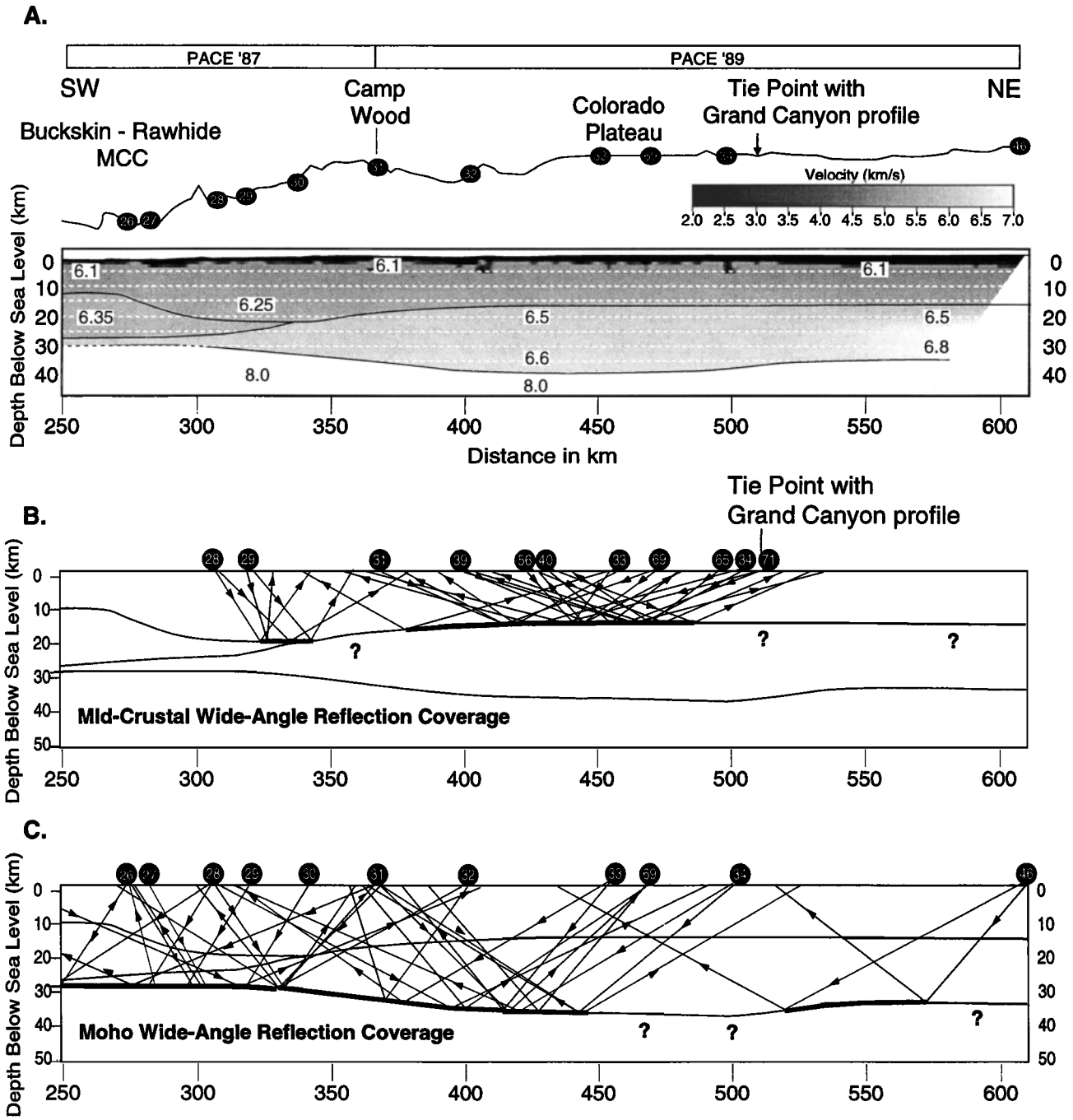

Figure 9. (a) Velocity model for the combined PACE 1987–1989 profiles. Depths are given relative to mean sea level. The model was developed through combination of finite difference travel time inversion for upper crustal velocity structure with finite difference forward modeling of secondary reflected arrivals from the middle crust and Moho. Velocities are shown in gray scale contours, and reflecting boundaries are outlined with black lines. See Figure 6 for a detailed model of the upper crust and the associated ray coverage. The PACE 1987 crustal model was generated originally using a forward ray tracing method [*Luetgert*, 1988] by *McCarthy et al.* [1991] and was reinterpreted with the finite difference techniques described in the text. Residual travel times between the calculated and data arrivals were essentially the same for the different techniques. A portion of the 1987 PACE model, beginning at 150 km, is shown here and is contiguous with the 1989 PACE profile. Details of the 1987–1989 model and techniques are discussed in the text. Reflection midpoint coverage ranges for the (b) middle crustal and (c) Moho reflectors in the PACE 1989 velocity model are shown. Heavy black lines on the model horizons show zones covered by reflections from at least one shot.

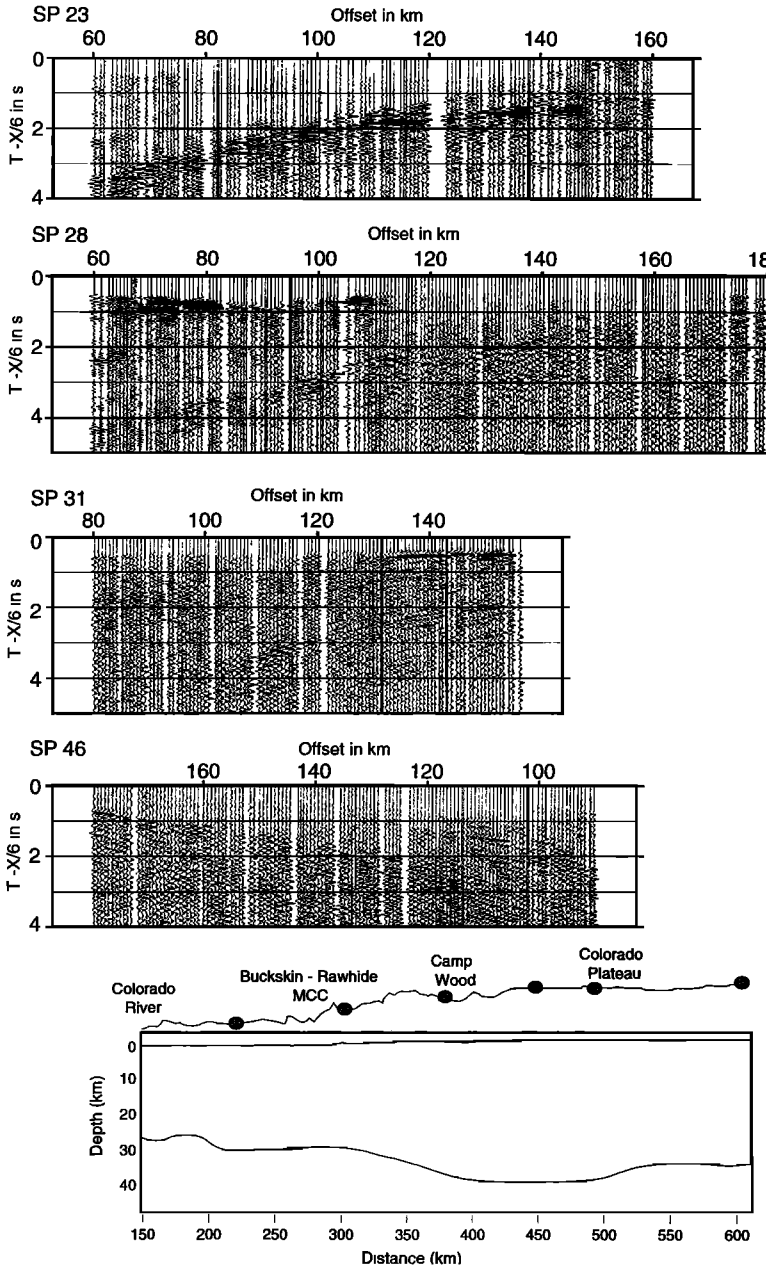

Figure 10. Four examples of *PmP* reflections recorded toward the northeast along the PACE 1987–1989 profiles. The strength of the *PmP* reflection can be seen declining into the background on the northernmost shots (31 and 46) that were recorded or detonated on the Colorado Plateau. The *PmP* phase is multicyclic on all the data and can be most plainly seen on shot 23, where the reflection and associated coda span about 1 s in travel time. We have chosen to consistently pick the top of the *PmP* phase on all the PACE data, because of the possibility that the coda do not originate from a layered lower crust but from along-path scattering and short-path multiples.

are required. The *PmP* phase on the PACE data is typically observed as a broad, multicyclic arrival that has coda. The source of the *PmP* coda may be along-path scattering and short-path multiples generated in the uppermost crust, or it may be the result of a transitional, interlayered crust-mantle boundary. On Figure 10, four examples of the *PmP* phase are shown from shots recorded from the southern Transition Zone (shot 23) to the Colorado Plateau (shot 46). The *PmP* arrival and coda can be plainly seen on the higher-amplitude shot records, and hints of it can be seen on the noisier records. If the apparent multicyclic nature of the *PmP* phase is the result of thin layers near the crust-mantle boundary, some uncertainty exists because the layers might be located in the upper mantle, the lower crust, or both. If the multicyclic *PmP* phase results from along-path scattering or near-surface conversions, then the breadth of the phase in time may not have a geological origin at the Moho.

Results of acoustic models for two shots (shot 23 recorded to the north in the Transition Zone and shot 46 recorded to the south on the Colorado Plateau) are shown in Plate 1. The plots are rasterized true-amplitude images of the data and synthetics. We find that many features of the real data can be dupli-

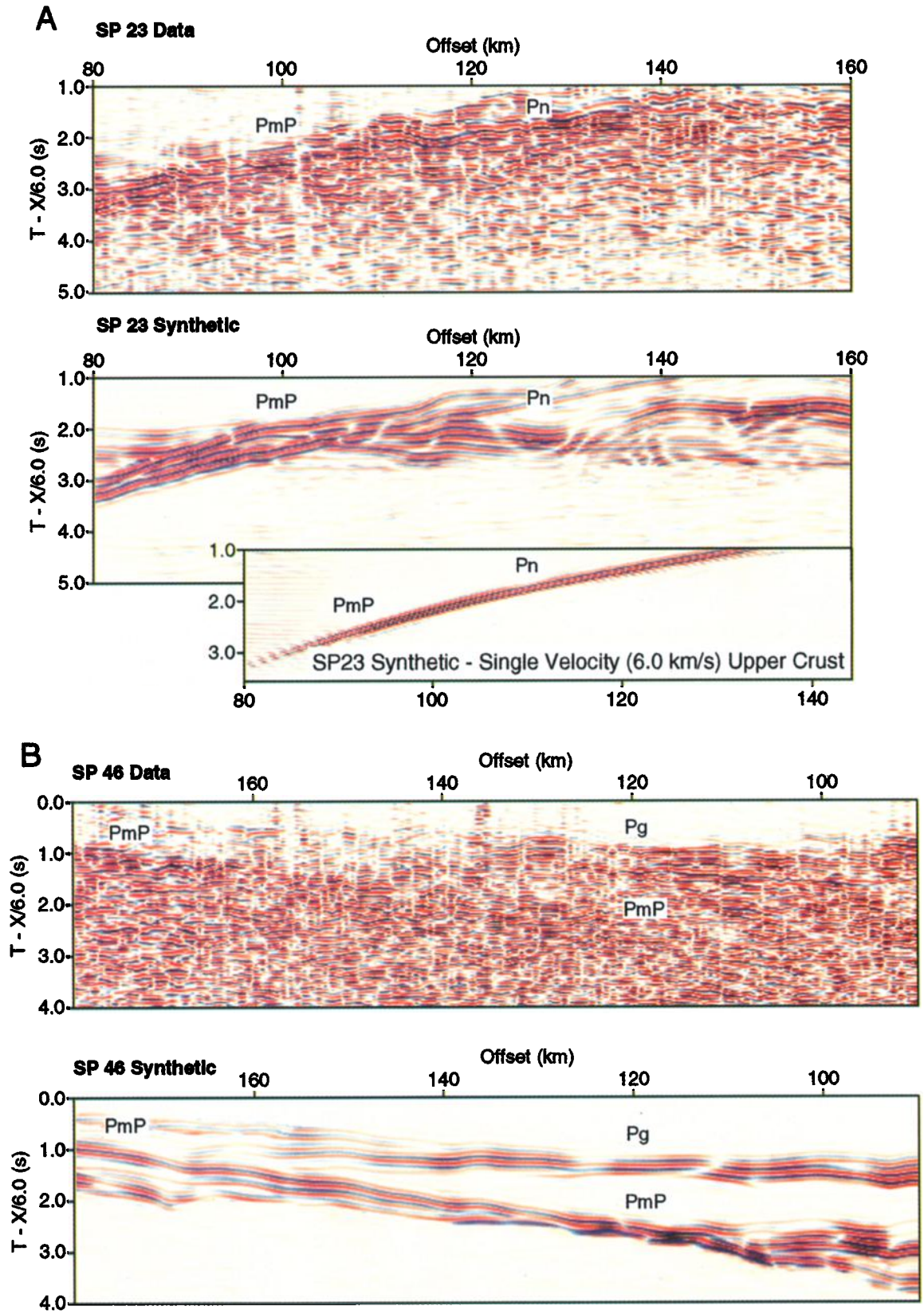

Plate 1. Comparisons of two shots, (a) shot 23 and (b) shot 46, recorded in the Transition Zone and on the Colorado Plateau, respectively, with acoustic models based on the velocity model shown in Figure 9. The *PmP* reflection and coda can be duplicated without a layered series of velocity contrasts at the Moho. The input velocity model includes the strong velocity contrasts in the uppermost crust. We believe that the apparent multicyclic nature of the *PmP* reflections is caused by scattering and reverberations in the upper crust because a model with the upper crust removed generates a simple *PmP* reflection, as shown in the inset model of Plate 1a. This point is reinforced by similar coda associated with the middle crustal reflections where observed. The crossover point of the *Pn* phase on shot 23 was well matched by the synthetic. *Pn* was not observed on shot 46.

cated by the acoustic models. These include the breadth in travel time of the *PmP* reflections and coda. We find that the primary features of the *PmP* reflections can be modeled without an interlayered Moho transition. We applied the same middle and deep crustal model for shot 23 with a single-velocity (6.0 km/s) upper crust which generated a much cleaner single-cycle *PmP* reflection (Plate 1, the uniform input upper crustal velocities caused the different *PmP* arrival times for this model). We thus attribute the observed and modeled *PmP* coda to reverberations within the upper crust, because the strongest velocity contrasts are there. The middle crustal reflections are associated with coda like the *PmP* reflections (Figure 8), which also suggests an upper crustal source for much of the scattering and multiple generation. This result is consistent with vertical-incidence studies of the Transition Zone and Colorado Plateau that did not observe an interlayered Moho transition [e.g., *Hauser et al.*, 1987; *Hauser and Lundy*, 1989; *Howie et al.*, 1991; *Parsons et al.*, 1992; *McCarthy and Parsons*, 1994]. There are later (~1–2 s behind *PmP*) choppy arrivals associated with the *PmP* reflection (particularly evident on shot 23 (Plate 1a)), that are not duplicated by the synthetic. We interpret this energy as *p* to *s* wave conversions that cannot be duplicated by the acoustic model. The amplitude and advance of the *Pn* phase ahead of *Pg* is well matched by the synthetic on shot 23. The acoustic modeling also duplicated the general appearance of the *Pg* and *PmP* phases on shot 46, although because it was an off-end shot, we have a less detailed upper crustal velocity model available because of reduced coverage in the upper crust (Figure 7). Reduced detail in the upper crustal velocity model near shot 46 caused some travel time mismatch in the *Pg* phase, as well as less *PmP* coda in the acoustic model as compared with the shot 23 model. Our results do not absolutely preclude the existence of an interlayered or transitional Moho boundary beneath the Transition Zone and Colorado Plateau but show that much if not all of the complexity of the *PmP* reflections can be explained by upper crustal structure.

A Crustal Model for the Grand Canyon Profile

A second crustal model (Figure 11) was generated from the Grand Canyon profile; this profile was confined to the interior of the Colorado Plateau and intersected the Colorado Plateau profile at its northern end (Figure 1). *Pg* arrivals from all 10 in-line shots were used to determine the upper crustal velocities, as depicted in Figure 11. The velocities of the near-surface sedimentary rocks are shown to increase rapidly from 2.5 to 5.9 km/s in the top 2 km of the crust. Crystalline basement below this depth has a much slower velocity gradient, increasing gradually from 5.9 to 6.1 km/s to a depth of 20 km. Midcrustal reflections were not resolvable from the Grand Canyon profile shots, but a velocity step from 6.1 to 6.4 km/s at 20 km depth was retained in the model to account for reflections from this horizon which were observed on the Colorado Plateau profile near the tie point between the two lines.

Determination of lower crustal and upper mantle structure on the Grand Canyon profile is based on two wide-angle reflections observed from shot 82 and a single wide-angle reflection observed from shot 83 (Figure 1). Because these three phases do not share common bottoming points and because shot 82 is offset from the receiver profile (and thus reciprocity cannot be checked), phase correlations are poorly constrained and lead to ambiguities in the deep crustal structure along the Grand Canyon profile. *Wolf and Cipar* [1993] have interpreted these data as showing a northwest tapering mafic lower crustal wedge (6.8–7.3 km/s), underlain everywhere by a flat Moho at 45 ± 3 km. Their interpretation is based on the correlation of the earlier of the two phases from shot 82 as the top of the mafic wedge in the lower crust and the later phase as the base, with the wide-angle reflection from shot 83 defining the tapered portion of the wedge. We offer an alternative interpretation in which the mafic wedge is replaced by a lateral change in crustal thickness, with the Moho increasing from 37 km in the south to 46 km in the north. Our model also includes a northward dipping discontinuity in the upper mantle localized beneath the San Francisco volcanic peaks. This model is based on the following observations and interpretations:

1. The intersecting Colorado Plateau velocity model (this paper) and an independent, receiver-function analysis of broadband teleseismic data [*Ruppert*, 1992] show the crustal thickness at the tie point with the Grand Canyon profile to be 37 km. Ray trace modeling of the earlier wide-angle reflection recorded from shot 82 also yields a 37 km depth estimate, and we thus correlate this phase with *PmP*.

2. The wide-angle reflection observed from shot 83 is a high-amplitude arrival followed by a ~1-s-thick packet of energy which we interpret to be coda [cf. *Wolf and Cipar*, 1993]. This reflection is similar in character to *PmP* recorded on other Colorado Plateau profile shots (e.g., shots 32, 33, 34, and 46), and we thus correlate the onset of this reflected energy with *PmP*.

3. Arrival times from this *PmP* reflection from shot 83 on the north end of the profile are later than those from shot 82 on the south end at similar shot-receiver offsets, suggesting a northward deepening of the Moho. The 46-km-thick crust modeled on the north end of the profile agrees well with an independent estimate of crustal thickness derived from receiver-function studies in northern Arizona [*Zandt et al.*, 1995]. Similarly, the 37-km-deep Moho at the updip terminus of this reflection agrees with the depth-to-Moho modeled from shot 82.

4. The deeper of the two wide-angle phases recorded from shot 82 is a band-limited, low-frequency (2–7 Hz) arrival which is difficult to identify on the shot record without low pass filtering (<7 Hz) (Figure 12). This is surprising given that the shot generated higher frequencies overall than any other shot (Figure 13). The band-limited nature of this arrival despite the presence of higher-frequency energy at the source requires one of two things: (1) either the energy from shot 82 was more rapidly attenuated at deep depths in the crust, or (2) the deep reflected phase corresponds to a longer-wavelength velocity transition which is transparent to higher-frequency energy. We can tentatively rule out observation 1 above, given that higher-frequency energy (5–15 Hz) is present in the record section and overprints the deep arrival but does not contribute to it. We thus determine that this reflection is different than all other deep reflections from beneath the Colorado Plateau and speculate that it may result from a second-order velocity discontinuity occurring over a thickness of hundreds of meters.

5. For reasons outlined in observations 1–4 above, we interpret the later wide-angle phase on shot 82 as an anomalous event originating in the upper mantle rather than at the base of the crust. To match the observed arrival times while maintaining 8.0 km/s upper mantle velocities above this layer, we introduced a northward dip on the interface. The velocity below the interface is unconstrained.

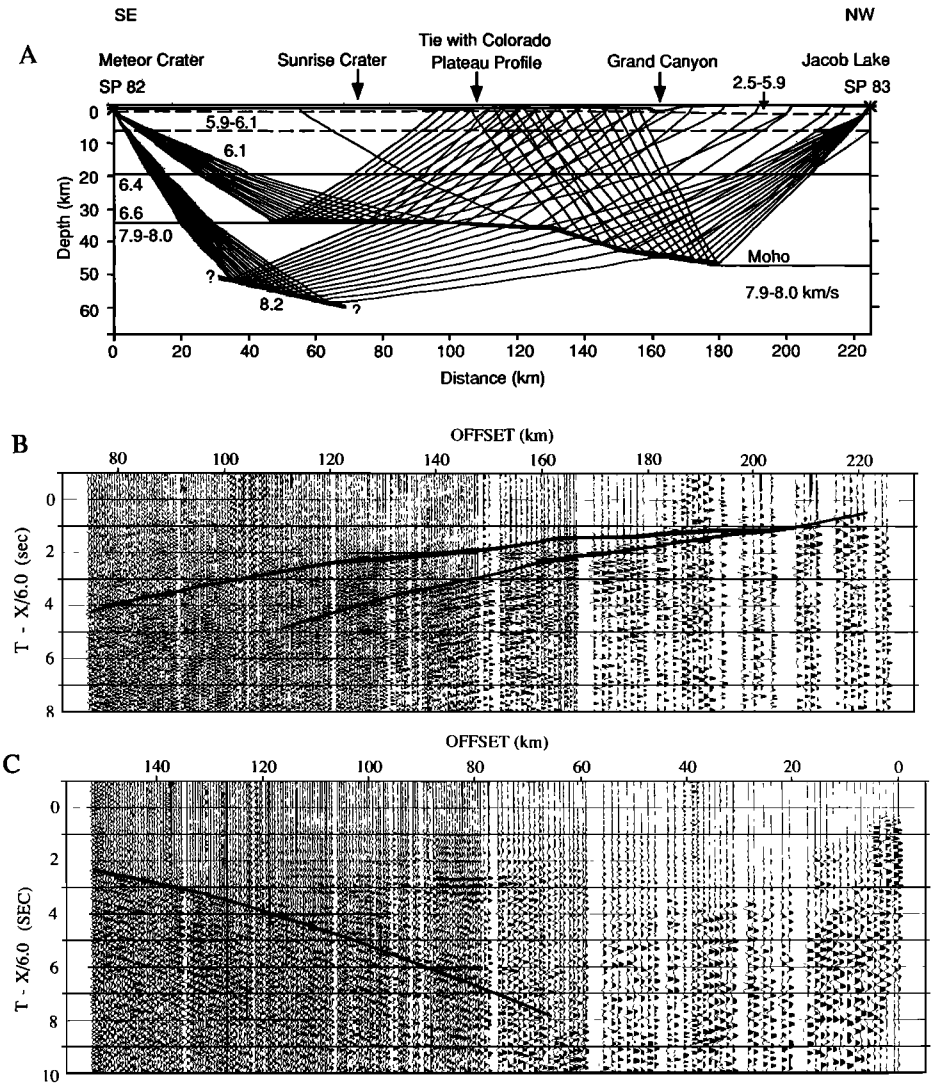

Figure 11. (a) Velocity model derived from the PACE 1989 Grand Canyon profile and data plots for shots (b) 82 and (c) 83. Ray coverage for the Moho and the upper mantle interface is shown in Figure 11a, and the corresponding calculated travel time curves are plotted in Figures 11b and 11c. Midpoint coverage is shown by the heavy black lines. Earlier *PmP* arrivals from the southeast off-end shot (82) suggest a thinner crust on the southeast end of the profile where it ties to the Colorado Plateau line. Later arrivals from the northwest shot (83) suggest a thicker crust to the north. The data were plotted with a low-frequency (0–7 Hz) band-pass filter. Details on the model are discussed in the text.

An important consequence of the Grand Canyon model is that we should expect to see a *Pn* phase crossing over and becoming a first arrival at about 120–140 km offset. We interpolated the Grand Canyon profile velocity model to a 100-m grid in the same way as the Colorado Plateau profile and generated a synthetic seismogram for shot 82 by solving the acoustic wave equation. We found that our Grand Canyon model predicts crossover of the *Pn* phase at about 135 km offset (Figure 14). We plotted the predicted arrival time of the *Pn* phase on the real data from shot 82 (Figure 14), but the high amplitudes of ambient noise present on that and the other seismograms recorded on the Colorado Plateau make the unequivocal identification of a weak phase like *Pn* impossible. We observe a very faint apparent phase at the approximate travel time appropriate for *Pn* but only across 4 or 5 traces at a time. Given the high-amplitude noise on the data and the low predicted amplitudes of the *Pn* phase, we feel that our model is still viable, despite the lack of an obvious *Pn* phase.

Implications of Errors Associated With the Analysis

Like nearly all long-offset crustal studies, our best control is on the uppermost crust, where we can measure the velocity directly from the travel times of direct and refracted waves (*Pg*). The travel time inversion for velocity converged to a solution with an RMS misfit of 0.06 s. We estimate the maximum picking error to be 0.1 s on the PACE data (for this error analysis we assume that the phase correlations were correct). The resolution of the inversion in travel time exceeds our confidence in our picks. Error ranges in the modeled velocity structure increase with depth. Beneath ~5–7 km depth the

velocities in the crust are constrained wholly by wide-angle reflections from the middle and lower crust. The nature of the middle crustal reflector as discussed in previous sections is likely disrupted and uneven along the profile, and reflections from it are not observed at all on the Grand Canyon profile. Modeling the middle crustal reflector as a discrete horizon creates an average travel time residual of 0.22 s, and a maximum of 0.3 s. These figures translate to maximum errors of ±0.09 km/s in velocity, or ±1.1 km in depth.

The *PmP* reflections observed on the PACE 1989 data were in general higher in amplitude than the middle crustal reflections and appear to have originated from a more coherent velocity contrast than the middle crustal horizon. This allowed us to generate a model with average travel time residuals (0.05 s) that were less than our estimated picking errors of 0.1 s. The maximum calculated residual travel time was 0.2 s for the *PmP* reflection. Lower crustal velocity structure is generally the most difficult aspect of a crustal model to constrain. We were limited to the observed curvature of the *PmP* reflections in time versus offset and the observations of multiple reversed recordings of *PmP* from different shot points to constrain the lower crustal velocity and crustal thickness. In Figure 15 the sensitivity of the calculated *PmP* phase curvature is shown for sample perturbations in the lower crustal velocities and Moho depths for two reversing shots (holding the upper crustal velocities and interfaces fixed). We find that a ±0.1 km/s shift in the average lower crustal velocity changes the shape of the calculated *PmP* curvature beyond the picking errors of 0.1 s. We also note that a thinner (~5-km-thick) high-velocity layer near the base of the crust of velocity >6.8 km/s changes the shape of the calculated *PmP* travel time curves beyond the picking errors (Figure 15). A ≤5-km-thick layer of velocity ≤6.8 km/s could lie above the Moho and not be detected. Thus the ~10-km-thick, 6.8 km/s layer modeled at the northeast end of the profile to fit the *PmP* arrival from shot 46 is just at the limit of our resolution. It is also important to note that while reversed wide-angle reflection coverage of the Moho is good from km 440 to the southwest, the model is developed from the unreversed shot 46 northeast of that point (Figure 9). Similarly, the Grand Canyon model was developed from shots 82 and 83 that were recorded in reversing directions but do not provide overlapping depth coverage on the Moho (Figure 11).

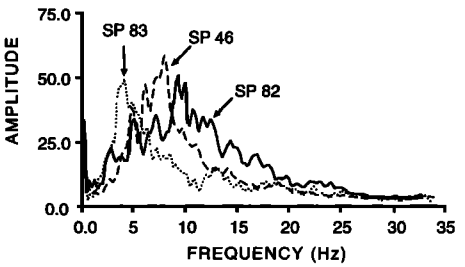

Figure 13. Amplitude spectra for the three wide-angle shotpoints recorded across the Colorado Plateau are shown. These spectra are computed using a 3-s window centered about the wide-angle reflected arrivals. The spectra are averaged over a 50-km-wide interval, and amplitudes are normalized. Both shots 46 and 82 were detonated in sandstone; these shots display higher frequencies than shot 83 which was detonated in limestone.

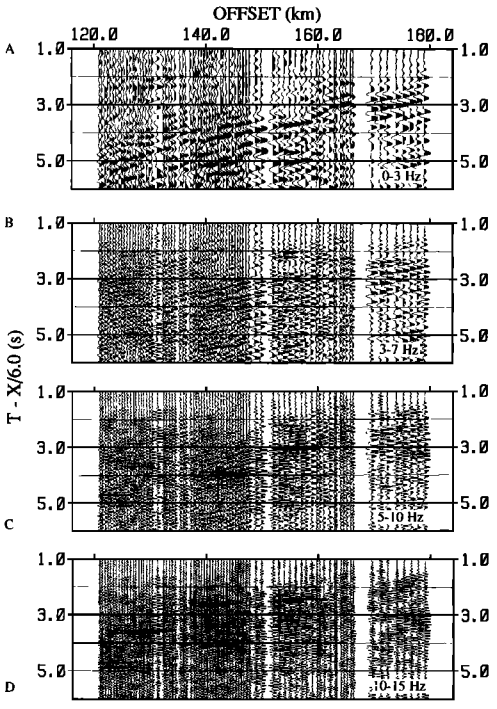

Figure 12. Filter panels for a 50-km-wide window of data recorded from shot 82. Shown are (a) 0–3 Hz, (b) 3–7 Hz, (c) 5–10 Hz, and (d) 10–15 Hz. The low-frequency display in Figure 12a reveals a prominent event ranging from 2 to 5 s and from 180 to 120 km offset, respectively. This event becomes progressively more obscured by higher-frequency energy in Figures 12b and 12c. Finally, by Figure 12d, only the onset of the higher-frequency energy (ranging from 1.5 to 2.5 s and from 180 to 120 km, respectively) stands out as a prominent feature in the data.

Geologic Implications of the Seismic Velocity Models

The Grand Canyon and Colorado Plateau velocity models have important implications for the compositional makeup of the plateau. Here we consider these implications, utilizing a laboratory data base of acoustic velocities measured at elevated confining pressures (up to 1 GPa) for a range of representative rock compositions [*Holbrook*, 1988]. We also correct for temperature effects, using two end-member geothermal gradients.

Surface heat flow on the southwestern margin of the Colorado Plateau near Flagstaff is lower than the Basin and Range to the west (<60 mW m^{-2} [*Lachenbruch and Sass*, 1978; *Sass et al.*, 1994]), despite the young San Francisco volcanic field (active within the past 1000 years [*Smiley*, 1958]) and the presence of an active magma chamber identified from teleseismic *p* wave residuals [*Stauber*, 1982]. *Lachenbruch and Sass* [1978] and *Sass et al.* [1994] have speculated that this relatively low surface heat flow is the result of hydrologic convection in the Coconino sandstone, leaving some ambiguity in the thermal conditions that exist at depth. Given the igneous activity evident along the plateau margin and the proximity to the high heat flow and active extension in the Arizona Transition Zone [e.g., *Sass et al.*, 1994], we reason that the lower crust/upper mantle temperatures are probably greater than or equal to those of the eastern Colorado Plateau. The lack of appreciable extension, however, suggests that these temperatures are still

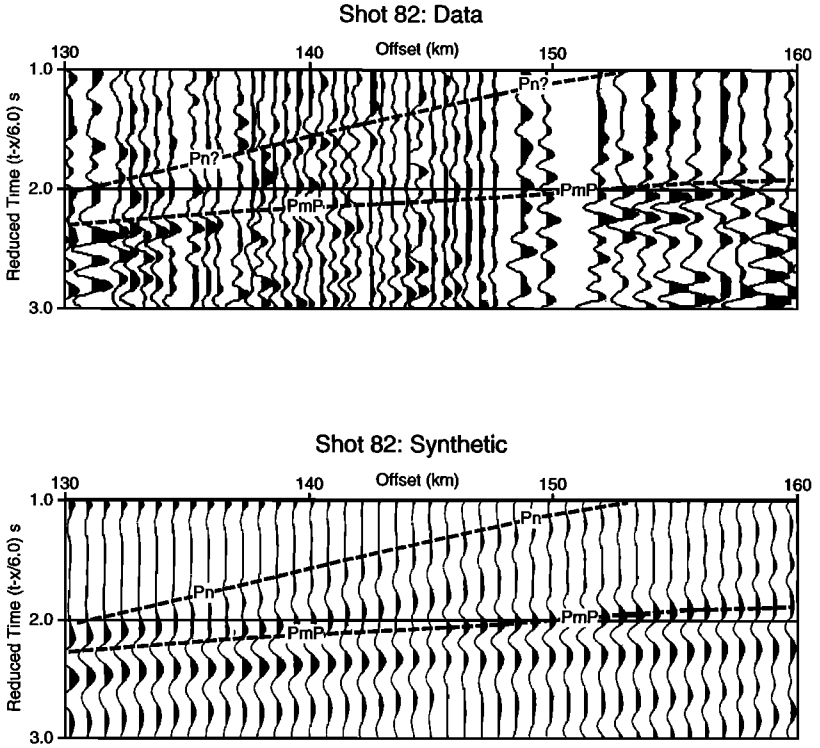

Figure 14. A comparison of a close-up window of the *PmP* reflection from shot 82 on the Grand Canyon profile (Figure 1) and a synthetic amplitude model for the *PmP* and *Pn* phases. The synthetic shows that the *Pn* phase is predicted to be relatively low-amplitude as compared with the *PmP* reflection. The travel time curve for the *Pn* phase as predicted by the synthetic is plotted on the real data. The high amplitudes of the ambient noise (which on some traces exceeds the *PmP* amplitudes) makes it very difficult to identify the *Pn* phase on the real data. There is some energy on some traces at the approximate time for *Pn*, but we feel that the high-amplitude noise bursts throughout the data collected on the Colorado Plateau make correlating and modeling such phases untenable.

not as high as those in the neighboring Transition Zone. For these reasons we infer a geothermal gradient ranging between 15° and 23°C km^{-1}, which corresponds to temperatures of 600° to 900°C, respectively, at 40 km depth. These temperature gradients are equivalent to the "stable" and "Basin and Range" geotherms defined by *Lachenbruch and Sass* [1978, Figure 9-5], and the upper end of our temperature estimate is in good agreement with the 850°–950°C upper mantle temper-

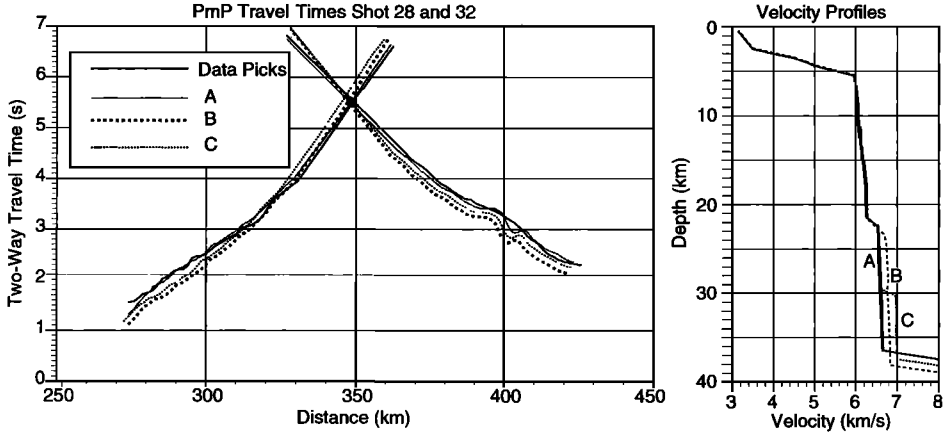

Figure 15. Model sensitivity to perturbations in lower crustal velocity for two example reversing *PmP* reflections. Model A is the velocity structure of our preferred model (Figure 9). We observe that a ±0.1 km/s variation in velocity can be accommodated by changing the depth to Moho slightly. Larger variations such as the 0.2 km/s increase in velocity shown in model B change the calculated curvature of the *PmP* reflection beyond the maximum 0.1 km/s picking error. We find that a 5-km-thick, or less, layer of varying velocity of up to ±0.2 km/s could go undetected in the lower crust but that a 0.4 km/s increase to 7.0 km/s in a 5-km-thick layer as shown in model C would produce detectable changes in the calculated *PmP* travel time curvature.

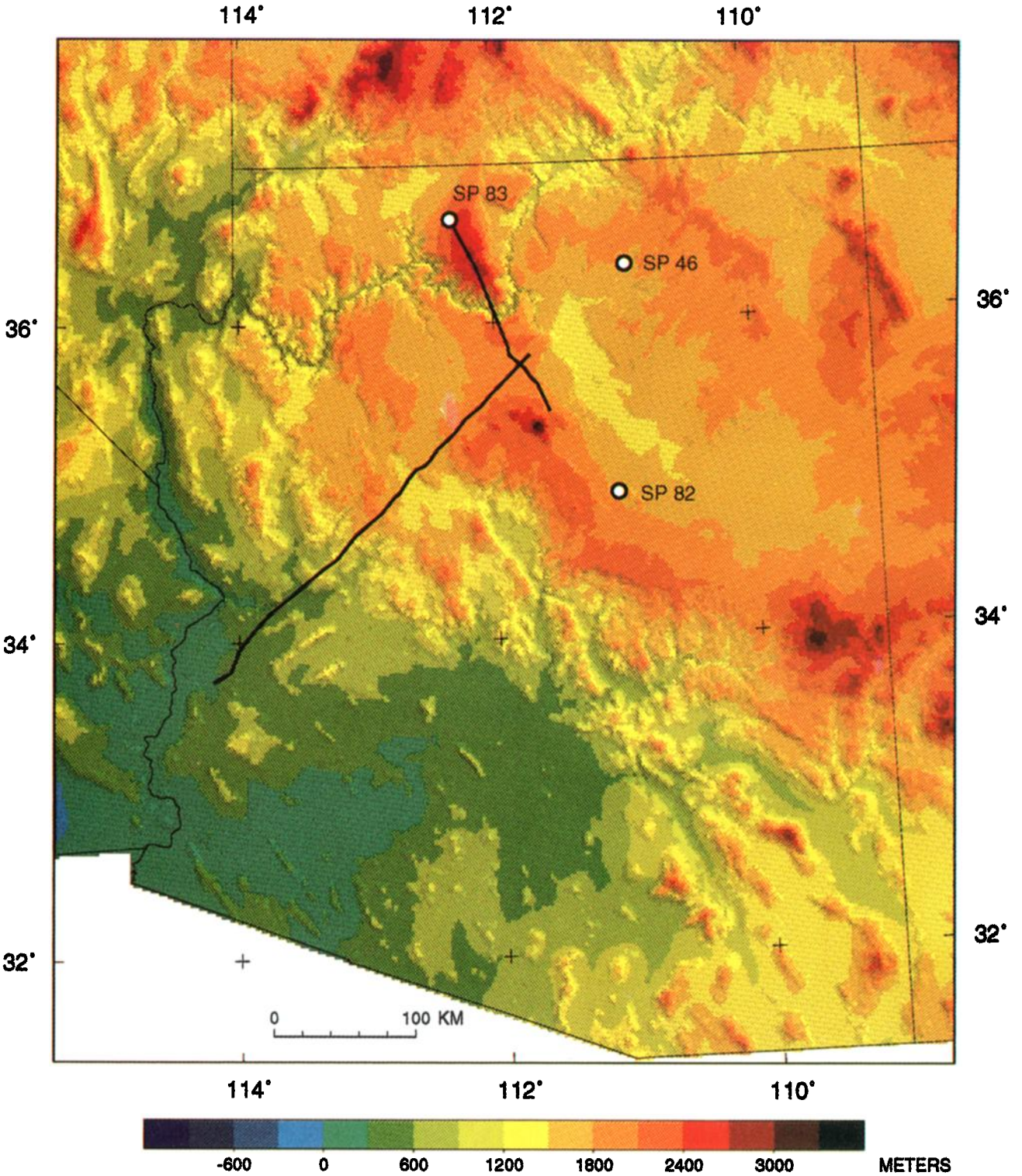

Plate 2. Topographic elevations in Arizona and surrounding regions. The locations of the two PACE refraction profiles are also shown. Note saucer-like shape of the plateau, with high elevations along the margins and lower elevations toward the interior.

atures determined from xenolith mineral assemblages in <1 Ma basalts erupted in the western Grand Canyon region [*Smith and Riter*, 1994; *Riter and Smith*, 1993]. We thus use these geotherms to correct the laboratory rock database for the effects of temperature before correlating seismic velocity to rock composition.

The velocity models for the two refraction profiles show slow velocities, increasing from 2.5 km/s to 5.9 km/s, in the shallow upper crust. These low velocities are confined to the upper 2 km of the models and correspond to the Paleozoic sedimentary rocks that comprise the Grand Canyon sequence. Below the near-surface sediments, seismic velocity increases gradually from 5.9 km/s to 6.2 km/s down to 20 km depth. Such velocities are compatible with quartzo-feldspathic rocks taken here to include granites, granodiorites, diorites, felsic schists, and gneisses. At the midcrustal discontinuity the velocity increases from 6.2 km/s to 6.5 km/s at a depth of 20 km. Velocities in the lower crust beneath this interface average 6.65 ± 0.1 km/s. These velocities are on the low end of typical mafic rocks (e.g., gabbro, amphibolite, and mafic granulite) for these estimated temperatures and pressures and suggest a mixture with more quartzo-feldspathic rocks (including diorites and granodiorites). The velocity again increases across the crust-mantle boundary from 6.8 to 8.0 km/s. Because *Pn* arrivals were not observed beneath the interior portion of the plateau, the 8.0-km/s velocities assigned to the upper mantle are extrapolated from reversed *Pn* arrivals across the southwest margin of the plateau and the northeastern Arizona Transition Zone. These upper mantle velocities are not unlike those estimated from local earthquake travel time studies (8.1 km/s [*Beghoul and Barazangi*, 1989] and 7.8–8.1 km/s [*Hearn et al.*, 1991]) and are compatible with a peridotite-rich upper mantle. The velocity and thickness of the upper mantle slab beneath the San Francisco volcanic peaks are unconstrained by the data.

Magmatism and Magmatic Underplating

The velocity models presented here do not include any velocities greater than 6.8 km/s in the lower crust and thus preclude any significant equilibrated underplating beneath the plateau, although young (<10 Ma) underplating may have low enough velocities. The average 6.6 km/s lower crustal velocities are suggestive of intermediate to mafic compositions and permit the addition of only limited amounts of dense, high-velocity (≥7.0 km/s) mafic material to the crust via magmatic underplating. On the basis of seismic velocities and seismic reflection patterns, *McCarthy and Parsons* [1994] estimated that a maximum of ~4 km of mafic material could have been intruded into the Arizona Transition Zone as a result of Tertiary magmatism and extension. Across the Colorado Plateau the lack of appreciable extension suggests that even lower amounts of Tertiary mafic material may have been intruded.

Our interpretation of lower crustal composition contrasts with that of *Wolf and Cipar* [1993], who model a 10-km-thick wedge of mafic material in the lower crust beneath the Grand Canyon profile. These investigators attribute the wedge to an episode of underplating of unknown age and project the mafic body northeast into the four corners region. Their regional correlation is based, in part, on the identification of two wide-angle phases recorded from shot 46 on the Grand Canyon profile. As with shot 82, they interpret the earlier of the two phases to be the top of the mafic underplated layer and the later phase to be the crust-mantle boundary at the base of the wedge. Our interpretation differs from that of *Wolf and Cipar* [1993] in that we see only a single wide-angle reflected phase from shot 46 followed by what we interpret to be nearly ~1 s of coda. Thus in our model the onset of reflected energy is correlated with *PmP* (not the top of a mafic underplate), and the trailing energy is the result of intracrustal scattering off of lateral velocity contrasts in the crust (see earlier section on *PmP* amplitude models for discussion of crustal scattering and coda).

Inherited Basement Structures

Several workers have noted the influence of the Proterozoic basement on the formation of monoclines during the Laramide orogeny [*Kelley*, 1955a, b; *Shoemaker et al.*, 1978]. *Davis* [1978] analyzed the geologic and spatial relationships of the plateau monoclines and concluded that they were controlled by a preexisting mosaic of basement fracture zones (oriented N20°W and N55°E) that were uplifted by reverse movements resulting from strong regional northeast directed compressive stress. *Davis* [1978] further concluded that one of these fracture zones, referred to as the Coconino lineament (Coconino salient of *Kelley* [1955a, b] and *Kelley and Clinton* [1960]), served as a major partitioning element in the basement and separated a northern zone of moderate compression (including the Grand View, Coconino Point, Echo Cliffs, Red Lake, Organ Rock, and Comb Ridge uplifts) from a southern zone of only mild compression (Black Mesa basin; Figure 16). In the vicinity of the East Kaibab and Grand View monoclines the Coconino lineament coincides with the Mesa Butte fault system of *Shoemaker et al.* [1978], who used satellite imagery to extrapolate the Mesa Butte fault system an additional 150 km to the southwest. Although the Mesa Butte fault is believed to have formed in the Proterozoic as a strike-slip fault, this feature is still active, as evidenced by historic seismicity and by offset volcanic deposits (15 to 0.5 Ma) from a suite of intermediate-composition volcanoes aligned along or near the lineament [*Shoemaker et al.*, 1978].

The PACE Colorado Plateau profile is largely coincident with the Coconino/Mesa Butte lineament, while the Grand Canyon profile is perpendicular to it. The down-to-the-north dip on the Moho modeled on the Grand Canyon profile begins approximately where this profile crosses the Coconino lineament. It is interesting to speculate that the lineament may be an upper crustal expression of a deep-seated change in lithospheric properties that dates back to the Proterozoic. Thus the development of plateau monoclines to the north and the Black Mesa Basin to the south may reflect the juxtaposition of two provinces with contrasting crustal thicknesses.

Crustal Thickening of the Plateau and Implications for Uplift

Many models have been proposed in the scientific literature to explain the Cenozoic uplift and tectonic evolution of the Colorado Plateau [e.g., *McGetchin and Merrill*, 1979; *Thompson and Zoback*, 1979; *Bird*, 1979, 1984, 1988; *McGetchin et al.*, 1980; *Chapman*, 1983; *Morgan and Swanberg*, 1985]. These different models fall largely into three basic groups: (1) uplift resulting from crustal thickening, (2) thermal expansion, or (3) delamination of mantle lithosphere [e.g., *Morgan and Swanberg*, 1985]. Because none of these mechanisms alone is capable of accounting for the 2 km uplift since the late Cretaceous [*Morgan and Swanberg*, 1985], most researchers invoke a combination of crustal thickening with either thermal expansion or

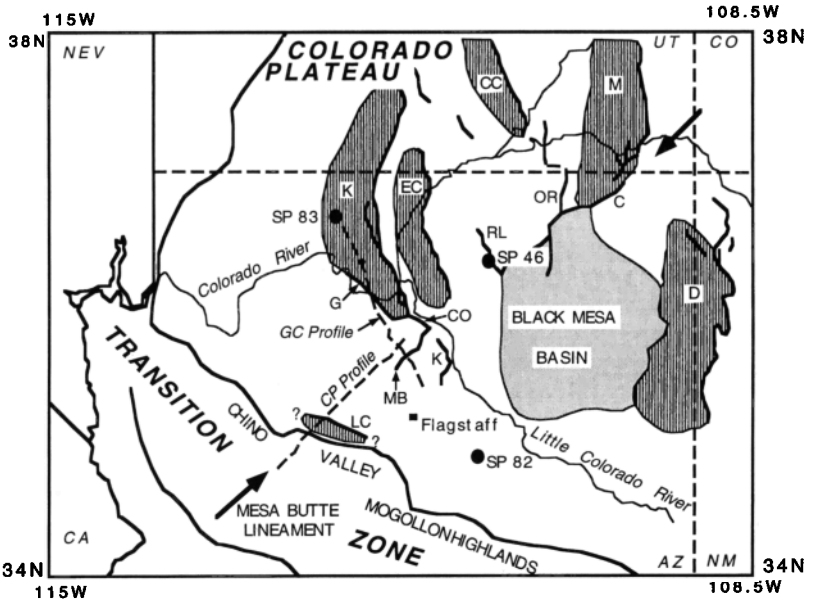

Figure 16. Index map showing the principal Laramide uplifts in northeastern Arizona and southern Utah. The locations of the 1989 PACE Grand Canyon (GC) and Colorado Plateau (CP) profiles are also shown (dashed lines) for reference. The Coconino Lineament marks the southern edge of several monoclines and block uplifts and also serves as the northern boundary of the Black Mesa Basin. The following abbreviations are used: C, Comb monocline; CC, Circle Cliffs uplift; CO, Coconino monocline; D, Defiance uplift; EC, Echo Cliffs uplift; G, Grandview monocline; K, Kaibab monocline; LC, Limestone Canyon monocline; M, Monument uplift; MB, Mesa Butte fault; OR, Organ Rock monocline; and RL, Red Lake monocline. Figure adapted from *Kelley and Clinton* [1960], *Krieger* [1965], and *Strahler* [1948].

lithospheric delamination [e.g., *Beghoul and Barazangi*, 1989]. We reexamine the evidence for crustal thickening below, with the PACE seismic refraction results supplemented with other geophysical and geological constraints. We focus primarily on the southwest margin of the plateau, where uplift is most recent, elevations are greatest, and where the crustal structure is best constrained.

Models that invoke crustal thickening can be subdivided into two categories: magmatic thickening and structural thickening. Our crustal model across the southwestern margin of the plateau indicates a crustal thickness of 37–42 km with lower crustal velocities of 6.6 ± 0.1 km/s. As noted above, these velocities are not compatible with underplating of significant quantities of dense mafic material to the base of the crust. Only a few km (~2 km) of high-velocity mafic material could have been underplated to the crust in this region without producing a recognizable signature in the velocity model [*McCarthy and Parsons*, 1994]. We thus estimate that only a minor amount of the recent uplift is the result of Tertiary magmatism.

Structural thickening via folding and thrusting is an alternative way to thicken the crust. Although the Colorado Plateau escaped much of the Laramide contractional deformation that characterized the bordering Basin and Range and Rocky Mountain provinces, the monoclines that were formed are indicative of at least a small percentage (~5%–10%) of Laramide crustal shortening and thickening. Most of these monoclines, however, are located north or east of the PACE Colorado Plateau refraction profile. This profile crosses only a minor monocline at the physiographic boundary of the plateau near Chino Valley (the Big Black Mesa anticline and associated Limestone Canyon Monocline of *Krieger* [1965]; Figure 16) and ends at the Grand View/East Kaibab uplift just prior to reaching the axis of the East Kaibab monocline. The Big Black Mesa anticline represents only a couple hundred meters of uplift, while the Grand View/East Kaibab uplift south of the Grand Canyon indicates 600–900 m of uplift (increasing to >1 km north of the Grand Canyon). Thus a maximum of a few kilometers of crustal thickening is suggested by these field relations. Interestingly, each of these regions also coincides with a region of thicker crust as shown in the Colorado Plateau and Grand Canyon velocity models. However, Laramide thrusting cannot account for all of this variation in crustal thickness, and it is possible that some of this interpreted variation predated the Laramide. This is supported by the observation that middle Cretaceous strata unconformably onlap Jurassic and early Cretaceous strata along the southern and western margins of the plateau, and thus the Mogollon highlands and the plateau's saucer-like shape (with higher elevations along the margins than in the interior of the plateau) must have existed at some reduced level prior to the Laramide [e.g., *Dickinson*, 1989].

In addition to crustal thickening via basement uplifts, *Bird* [1984, 1988] proposed a second mechanism to account for the unusually large crustal thicknesses reported primarily beneath the Rocky Mountains and Great Plains regions. He advocated crustal thickening via subhorizontal shear at the base of the crust, resulting from horizontal drag forces exerted by the flat Farallon slab on the North American plate. *Beghoul and Barazangi* [1989] applied this model to the Colorado Plateau and concluded that lower crustal shear was responsible for the thickened crust and the Cenozoic uplift of the plateau. Their conclusion, however, was dependent on the *Hauser and Lundy* [1989] interpretation that the plateau crust was ≥50 km thick. The latter has not been substantiated by the PACE refraction

results, which instead have been modeled with crustal thicknesses that are typically ≤45 km. We thus conclude that if the flat Farallon slab exerted any horizontal drag forces on the Colorado Plateau lower crust during the Laramide, this probably resulted in a net thinning of the crust (accompanied by an eastward translation of crustal material beneath the eastern Colorado Plateau and Rio Grande rift regions), rather than thickening in this location.

The lack of a thick crustal root beneath the southwest margin of the plateau suggests a mantle contribution to uplift. *Parsons and McCarthy* [1995] utilized a regional grid of seismic profiles in northern and central Arizona combined with observed elevations to estimate the mantle contribution to uplift. Their results suggest that the crust is not thick enough to support its height isostatically across much of the region, requiring an anomalous upper mantle. The region of anomalous upper mantle extends as far west as the Transition Zone and provides an explanation for the locally high elevations (often exceeding that of the plateau) despite ongoing extension. Although the mantle contribution to uplift beneath the Flagstaff region may be smaller than that inferred by *Parsons and McCarthy* [1995], if the thicker crustal model of *Wolf and Cipar* [1993] is correct, regionally the mantle still must play a dominant role in order to account for the high elevations across the Colorado Plateau–Basin and Range transition.

Conclusions

The Colorado Plateau has been an intriguing and yet elusive target for geologists determined to unravel its recent history and explain its present elevation. The PACE 1989 refraction studies significantly advance our understanding of the plateau's crustal structure, although many questions still remain. Modeling of the 1987 and 1989 Colorado Plateau profile reveals a progressive increase in crustal thickness across the Basin and Range–Colorado Plateau transition, ranging from ~30 km beneath the metamorphic core complex belt to 42 km beneath the southwest margin of the plateau. Farther inboard, 100–150 km northeast of the physiographic boundary of the plateau, the crustal thickness appears to decrease slightly to between 37 and 40 km. The perpendicular Grand Canyon profile crosses the northeastern portion of the Colorado Plateau profile and is located strictly within the Colorado Plateau physiographic province. On the basis of modeling of these data, we estimate that the crust is 45–48 km thick beneath the Kaibab uplift on the north rim of the Grand Canyon, decreasing to 37 km on the southeast end of the profile in the vicinity of Flagstaff. Because only two shots recorded wide-angle reflections from the Moho on the Grand Canyon profile, crustal thickness is poorly constrained. *Wolf and Cipar* [1993] have interpreted these same data quite differently. In their model they showed a northward pinching lower crustal wedge of high velocity, mafic material, underlain everywhere by a flat Moho at 45 ± 3 km.

The primary difference between our model and that of *Wolf and Cipar* [1993] is the interpretation of the deeper phase identified on shot 82. *Wolf and Cipar* [1993] modeled this phase as the flat-lying base of a 10-km-thick, 7.0 km/s wedge. Without overlapping subsurface coverage from a reversing shot, however, there is no constraint on the dip of this interface. We instead elected to model this reflection as a northward dipping discontinuity in the upper mantle. We matched the observed 7.0 km/s velocities by shooting rays downdip through 8.0 km/s rocks. Our model thus ties with the intersecting Grand Canyon profile (8.0 km/s velocities at 37 km depth) and predicts a much thinner crust south of the Grand Canyon.

Our PACE crustal thickness estimates are broadly compatible with the early seismic estimates of crustal thickness determined for the Arizona portion of the Colorado Plateau. On the basis of two reversing wide-angle shots, *Roller* [1965] determined a 40–43 km thick crust for northeastern Arizona (cf. *Wolf and Cipar* [1993, Figure 1], who estimate a 45- to 48-km-thick crust). *Warren* [1969] arrived at a similar estimate of ~40 km based on a multisource profile that crossed the southwestern margin of the plateau (Figure 1). More recently, *Ruppert* [1992] estimated a 37-km-thick crust based on a receiver-function study situated near the tie point of the two PACE profiles, and *Zandt et al.* [1995] estimated a 45-km-thick crust at 37°N latitude using the same technique. Thus, although local variations in crustal thickness are implied by these different results, the variation is relatively small, and there is little evidence that the crust is thicker than 45 km [cf. *Hauser and Lundy*, 1989], except locally beneath the Kaibab uplift in northernmost Arizona.

Seismic velocities are uniform across Transition Zone–Colorado Plateau transition, suggesting that the two provinces differ only in terms of percent extension. This contrasts with crustal structure models in northernmost Arizona and southern Nevada, where the Colorado Plateau crust is shown to be more mafic than its Basin and Range counterpart [*Zandt et al.*, 1995]. We speculate that without a change in composition and physical properties to focus extensional stresses, crustal thinning in central Arizona occurred over a much longer wavelength, resulting in a 100-km-wide transition zone separating the highly extended metamorphic core complexes from the relatively unextended Colorado Plateau.

The refraction results document that the crustal thickness of the Colorado Plateau is not uniform but varies by as much as ~15% regionally. This variability is also reflected in surface topography, which ranges between 1350 and 3000 m across the Arizona portion of the Colorado Plateau (Plate 2), with the highest regions apparently underlain by the thickest crust. For example, the 2750-m elevations of the North rim of the Grand Canyon are associated with ≥45-km crustal thickness locally, while the 1400-m elevations northeast of Flagstaff (just east of the tie-point in the two refraction profiles) are associated with 37- to 40-km-thick crust. Although some of this variability was undoubtedly introduced during the Laramide, stratigraphic relations suggest that the Mogollon rim has been high relative to the interior of the plateau since at least the early Cretaceous [*Dickinson*, 1989].

Inversions for upper mantle velocity structure using *Pn* arrivals from earthquake sources also provide insights into the deep lithospheric makeup of the plateau. *Hearn et al.* [1991] recently concluded that the velocity of the upper mantle beneath the Colorado Plateau could not be characterized by a single value but instead ranged between 7.8 and 8.1 km/s. This variability is not surprising given the variations in uplift and magmatism across the plateau. It is also possible, however, that some of this upper mantle variability in seismic velocity is an artifact of crustal thickness variations. If the latter are not accounted for, the inversion is likely to map them into variations in the upper mantle thereby affecting the calculated upper mantle seismic velocity.

The Colorado Plateau is unique in that it is perhaps the only region in the western cordillera that has avoided significant deformation since the Precambrian. Thus it is one of the few

areas where the Proterozoic lithospheric discontinuities are still preserved and have not been significantly overprinted. The northward deepening Moho ramp modeled across the Grand Canyon profile may be one such structure (Figure 11). This feature is broadly coincident with the Coconino/Mesa Butte lineament, a prominent northeast striking fault that has been active intermittently since the Precambrian. The Coconino/Mesa Butte lineament has apparently served as a major partitioning element in the basement, separating a northern zone of moderate compression from a southern zone of only mild compression [*Davis*, 1978]. We thus speculate that this Proterozoic lineament may be controlled by, or serve as the upper crustal expression of, this north-south change in crustal thickness.

The processes controlling the uplift of the Colorado Plateau were first contemplated by *Dutton* [1892, p. 30], when he inferred that "the cause which elevates the land involves expansion." Since then many investigators have looked to the mantle as a possible source of this uplift [e.g., *Bird*, 1979; *Thompson and Zoback*, 1979; *McGetchin and Merrill*, 1979; *Morgan and Swanberg*, 1985], invoking a variety of different geologic mechanisms to explain the present day elevations. The PACE lithospheric investigation represents another step forward in our understanding of the Colorado Plateau in that it has allowed us to separate out the mantle and crustal contributions to uplift [*Parsons and McCarthy*, 1995]. Many critical questions still remain, however, such as the thickness of the mantle lithosphere, the density and temperature distribution in the upper mantle, and the changes in the upper mantle resulting from long-term subduction of oceanic lithosphere along the margin of western North America. Additional seismic and xenolith studies focused on the upper mantle are needed to assess these variables and to provide added insights into the evolution of this fascinating geologic province.

Acknowledgments. The PACE 1989 experiment was unique in terms of the collaborative nature of the study. We would like to express a special thanks to the Navajo and Hopi Nations and the Grand Canyon National Park for providing special access to protected lands. We thank George Billingsley, John Cipar, Gary Fuis, Zoltan Hajnal, Steve Harder, Gordon Haxel, Keith Howard, John Howie, Roy Johnson, Randy Keller, Art Lachenbruch, Ivo Lucchitta, John Sass, Robert Simpson, George Thompson, and Lorraine Wolf for their numerous and varied contributions to this study. Funding was provided by five principal organizations: the U.S. Geological Survey's Deep Continental Studies Program, the Air Force Geophysics Laboratory (AFGL), the University of Texas at El Paso (through a grant from the AFGL), the Gas Research Institute, and the National Science Foundation. The Geological Survey of Canada graciously provided 150 PRS1 and PRS4 recorders used in this study. The USGS, AFGL, and the University of Texas at El Paso provided primary funding for the two refraction/wide-angle reflection profiles. Reviews by Kevin Furlong, Erik B. Goodwin, John M. Howie, David James, Jim Luetgert, Kate C. Miller, Walter Mooney, Steve Reynolds, and two anonymous reviewers greatly improved this manuscript.

References

Beghoul, N., and M. Barazangi, Mapping high *Pn* velocity beneath the Colorado Plateau constrains uplift models, *J. Geophys. Res.*, *94*, 7083–7104, 1989.

Bird, P., Continental delamination and the Colorado Plateau, *J. Geophys. Res.*, *84*, 7561–7571, 1979.

Bird, P., Laramide crustal thickening event in the Rocky Mountain foreland and Great Plains, *Tectonics*, *3*, 741–758, 1984.

Bird, P., Formation of the Rocky Mountains, western United States: A continuum computer model, *Science*, *239*, 1501–1507, 1988.

Chapman, D. S., Colorado Plateau: Thermal-tectonic evolution, paper presented at IUGG Inter-disciplinary Symposia, Hamburg, Germany, Aug. 15–27, 1983.

Davis, G. H., Monocline fold pattern of the Colorado Plateau, in *Laramide Folding Associated With Basement Block Faulting in the Western United States*, edited by V. Matthews III, *Mem. Geol. Soc. Am.*, *151*, 215–233, 1978.

Dickinson, W. R., Tectonic setting of Arizona through geologic time, in *Geologic Evolution of Arizona*, edited by J. P. Jenney and S. J. Reynolds, *Ariz. Geol. Soc. Dig.*, *17*, 1–16, 1989.

Dutton, C. E., On some of the greater problems of physical geology, *Phlos. Soc. Wash.*, *11*, 51–64, 1892.

Goodwin, E. B., and J. McCarthy, Composition of the lower crust in west-central Arizona from three-component seismic data, *J. Geophys. Res.*, *95*, 20,097–20,109, 1990.

Hauser, E. C., and J. Lundy, COCORP deep reflections: Moho at 50 km (16 s) beneath the Colorado Plateau, *J. Geophys. Res.*, *94*, 7071–7081, 1989.

Hauser, E. C., J. Gephart, T. Latham, L. Brown, S. Kaufman, J. Oliver, and I. Lucchitta, COCORP Arizona transect: Strong crustal reflections and offset Moho beneath the transition zone, *Geology*, *15*, 1103–1106, 1987.

Hearn, T. M., N. Beghoul, and M. Barazangi, Tomography of the western U.S. from regional arrival times, *J. Geophys. Res.*, *96*, 16,369–16,381, 1991.

Holbrook, W. S., Wide-angle seismic studies of crustal structure and composition in Nevada, California, and southwest Germany, Ph.D. thesis, 214 pp., Stanford Univ., Stanford, Calif., 1988.

Hole, J. A., and B. C. Zelt, 3-D finite-difference reflection travel times, *Geophys. J. Int.*, *121*, 427–434, 1995.

Howie, J. M., T. Parsons, and G. A. Thompson, High-resolution *P*- and *S*-wave deep crustal imaging across the edge of the Colorado Plateau, USA: Increased reflectivity caused by initiating extension, in *Continental Lithosphere: Deep Seismic Reflections, Geodyn. Ser.*, vol. 22, edited by R. Meissner et al., pp. 21–29, AGU, Washington, D. C., 1991.

Humphreys, E., and R. W. Clayton, Adaptation of back projection tomography to seismic travel time problems, *J. Geophys. Res.*, *93*, 1073–1085, 1988.

Kelley, V. C., Regional tectonics of the Colorado Plateau and relationship to the origin and distribution of uranium, *Univ. N. M. Publ. Geol.*, *5*, 120 pp., 1955a.

Kelley, V. C., Monoclines of the Colorado Plateau, *Geol. Soc. Am. Bull.*, *66*, 789–804, 1955b.

Kelley, V. C., and N. J. Clinton, Fracture systems and tectonic elements of the Colorado Plateau, *Univ. N. M. Publ. Geol.*, *6*, 104 pp., 1960.

Krieger, M. H., Geology of the Prescott and Paulden quadrangles, Arizona, *U.S. Geol. Surv. Prof. Pap.*, *467*, 127 pp., 1965.

Lachenbruch, A. H., and J. H. Sass, Models of an extending lithosphere and heat flow in the Basin and Range Province, in *Cenozoic Tectonics and Regional Geophysics of the Western Cordillera*, edited by R. B. Smith and G. P. Eaton, *Mem. Geol. Soc. Am.*, *152*, 209–250, 1978.

Larkin, S. P., J. McCarthy, and G. S. Fuis, Data report for the PACE 1987 seismic refraction survey, west-central Arizona, *U.S. Geol. Surv. Open File Rep.*, *88-694*, 95 pp., 1988.

Lees, J. M., and R. S. Crosson, Tomographic inversion for three-dimensional velocity structure at Mount St. Helens using earthquake data, *J. Geophys. Res.*, *94*, 5716–5728, 1989.

Luetgert, J. J., Users manual for RAY84/R83PLT: Interactive two-dimensional raytracing/synthetic seismogram package, *U.S. Geol. Surv. Open File Rep.*, *88-238*, 55 pp., 1988.

McCarthy, J., and T. Parsons, Kinematic model for the Cenozoic evolution of the Colorado Plateau: Basin and Range transition from coincident seismic refraction and reflection data, *Geol. Soc. Am. Bull.*, *106*, 747–759, 1994.

McCarthy, J., S. P. Larkin, G. S. Fuis, R. W. Simpson, and K. A. Howard, Anatomy of a metamorphic core complex: Seismic refraction/wide-angle reflection profiling in southeastern California and western Arizona, *J. Geophys. Res.*, *96*, 12,259–12,291, 1991.

McCarthy, J., W. Kohler, and E. Criley, Data report for the 1989 PACE refraction survey, northern Arizona, *U.S. Geol. Surv. Open File Rep.*, *94-138*, 88 pp., 1994.

McGetchin, T. R., and R. B. Merrill (Eds.), Plateau uplift: Mode and mechanism, *Tectonophysics*, *61*, 336 pp., 1979.

McGetchin, T. R., K. C. Burke, G. A. Thompson, and R. A. Young, Mode and mechanism of plateau uplifts, in *Dynamics of Plate Interiors, Geodyn. Ser.*, vol. 1, edited by A. W. Bally, P. L. Bender, T. R. McGetchin, and R. I. Walcott, pp. 99–110, AGU, Washington, D. C., 1980.

Morgan, P., and C. A. Swanberg, On the Cenozoic uplift and tectonic stability of the Colorado Plateau, *J. Geodyn.*, *3*, 39–63, 1985.

Paige, C. C., and M. A. Saunders, LSQR: An algorithm for sparse linear equations and sparse least squares, *Trans. Math. Software*, *8*, 43–71, 1982.

Parsons, T., and J. McCarthy, The active southwest margin of the Colorado Plateau: Uplift of mantle origin, *Geol. Soc. Am. Bull.*, *107*, 139–147, 1995.

Parsons, T., J. M. Howie, and G. A. Thompson, Seismic constraints on the nature of lower crustal reflectors beneath the extending southern Transition Zone of the Colorado Plateau, Arizona, *J. Geophys. Res.*, *97*, 12,391–12,407, 1992.

Prodehl, C., Crustal structure of the western United States, *U.S. Geol. Surv. Prof. Pap.*, *1034*, 74 pp., 1979.

Riter, J. C. A., and D. Smith, Analysis of Grand Canyon Cr-Diopside group spinel peridotite and pyroxenite xenoliths (abstract), *Eos Trans. AGU*, *74*(43), Fall Meet. Suppl., 637, 1993.

Roller, J. C., Crustal structure in the eastern Colorado Plateaus province from seismic refraction measurements, *Geol. Soc. Am. Bull.*, *55*, 107–119, 1965.

Ruppert, S. D., Tectonics of western North America, Ph.D. thesis, 217 pp., Stanford Univ., Stanford, Calif., 1992.

Sass, J. H., A. H. Lachenbruch, S. P. Galanis Jr., P. Morgan, S. S. Priest, T. H. Moses Jr., and R. J. Munroe, Thermal regime of the southern Basin and Range province, 1, Heat flow data from Arizona and the Mojave Desert of California and Nevada, *J. Geophys. Res.*, *99*, 22,093–22,119, 1994.

Shaw, P. R., and J. A. Orcutt, Waveform inversion of seismic refraction data and applications to young Pacific crust, *Geophys. J. R. Astron. Soc.*, *82*, 375–414, 1986.

Shoemaker, E. M., R. L. Squires, and M. J. Abrams, Bright Angel and Mesa Butte fault systems of northern Arizona, in *Cenozoic Tectonics and Regional Geophysics of the Western Cordillera*, edited by R. B. Smith and G. P. Eaton, *Mem. Geol. Soc. Am.*, *152*, 341–367, 1978.

Smiley, T. L., The geology and dating of Sunset Crater, Flagstaff, Arizona, in *Black Mesa Basin, northeastern Arizona, Field Conf. Guideb. N. M. Geol. Soc.*, 9th, 186–190, 1958.

Smith, D., and J. C. A. Riter, Mantle xenoliths and the Colorado Plateau, *Geol. Soc. Am. Abstr. Programs*, *26*, 63–64, 1994.

Stauber, D. A., Two-dimensional compressional wave velocity structure under San Francisco volcanic field, Arizona, from teleseismic *P* residual measurements, *J. Geophys. Res.*, *87*, 5451–5459, 1982.

Strahler, A. N., Geomorphology and structure of the West Kaibab fault zone and Kaibab Plateau, Arizona, *Geol. Soc. Am. Bull.*, *59*, 513–540, 1948.

Thompson, G. A., and M. L. Zoback, Regional geophysics of the Colorado Plateau, *Tectonophysics*, *61*, 149–181, 1979.

Vidale, J. E., Finite-difference calculation of traveltimes, *Bull. Seismol. Soc. Am.*, *78*, 2062–2076, 1988.

Vidale, J. E., Finite-difference calculation of traveltimes in three dimensions, *Geophysics*, *55*, 521–526, 1990.

Warren, D. H., A seismic-refraction survey of crustal structure in central Arizona, *Geol. Soc. Am. Bull.*, *80*, 257–282, 1969.

Wilshire, H. G., Lithology and evolution of the crust-mantle boundary region in the southwestern Basin and Range province, *J. Geophys. Res.*, *95*, 649–665, 1990.

Wilson, J. M., and G. S. Fuis, Data report for the Chemehuevi, Vidal, and Dutch Flat lines: PACE seismic-refraction survey, southeastern California, and western Arizona, *U.S. Geol. Surv. Open File Rep.*, *87-86*, 75 pp., 1987.

Wilson, J. M., J. McCarthy, R. A. Johnson, and K. A. Howard, An axial view of a metamorphic core complex: Crustal structure of the Whipple and Chemehuevi Mountains, southeastern California, *J. Geophys. Res.*, *96*, 12,293–12,311, 1991.

Wolf, L. W., and J. J. Cipar, Through thick and thin: A new model for the Colorado Plateau from seismic refraction data from Pacific to Arizona Crustal Experiment, *J. Geophys. Res.*, *98*, 19,881–19,894, 1993.

Zandt, G., S. C. Myers, and T. C. Wallace, Crust and mantle structure across the Basin and Range–Colorado Plateau boundary at 37°N latitude and implications for Cenozoic extensional mechanism, *J. Geophys. Res.*, *100*, 10,529–10,548, 1995.

C. J. Ammon, Department of Earth and Atmospheric Sciences, Saint Louis University, Saint Louis, MO 63103.

H. M. Benz, U.S. Geological Survey, P.O. Box 25046, Denver, CO 80225.

E. E. Criley, W. M. Kohler, J. McCarthy, and T. Parsons, U.S. Geological Survey, 345 Middlefield Road, MS 999, Menlo Park, CA 94025. (e-mail: mccarthy@octopus.wr.usgs.gov)

J. A. Hole, Department of Geophysics, Stanford University, Stanford, CA 94305.

(Received September 28, 1995; revised November 29, 1995; accepted December 7, 1995.)